AD-A043 185 OWENS-ILLINOIS INC TOLEDO OHIO CORPORATE TECHNOLOGY DIV F/G 20/5
INVESTIGATION OF BROAD-BAND EMITTERS AS POTENTIAL LASING IONS B--ETC(U)
JUL 77 C F RAPP, N L BOLING, C M CARLEN F44620-76-C-0088
UNCLASSIFIED AFOSR-TR-77-0959 NL

1 OF 1
AD A043185

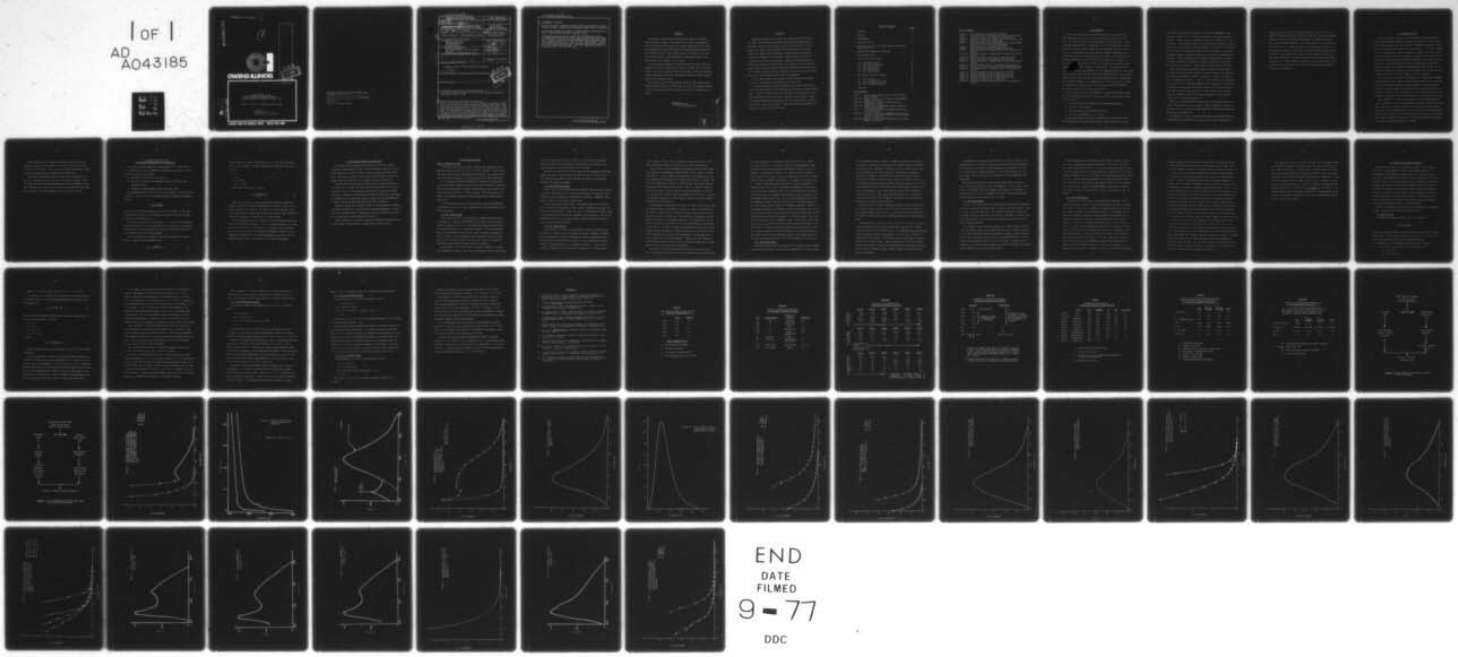

END
DATE FILMED
9-77
DDC

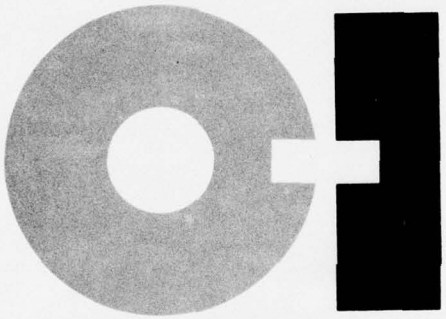

OWENS-ILLINOIS

INTERIM REPORT ON THE INVESTIGATION OF BROAD-BAND EMITTERS AS POTENTIAL LASING IONS BETWEEN 0.5 AND 1.0 μm

Charles F. Rapp, N. L. Boling, Cloyce M. Carlen

July 1977

A REPORT FROM THE TECHNICAL CENTER TOLEDO, OHIO, 43666

AIR FORCE OFFICE OF SCIENTIFIC RESEARCH (AFSC)
NOTICE OF TRANSMITTAL TO DDC
This technical report has been reviewed and is
approved for public release IAW AFR 190-12 (7b).
Distribution is unlimited.
A. D. BLOSE
Technical Information Officer

Unclassified

SECURITY CLASSIFICATION OF THIS PAGE (When Data Entered)

REPORT DOCUMENTATION PAGE	READ INSTRUCTIONS BEFORE COMPLETING FORM
1. REPORT NUMBER: AFOSR-TR-77-0959	2. GOVT ACCESSION NO. / 3. RECIPIENT'S CATALOG NUMBER
4. TITLE (and Subtitle): ~~INTERIM REPORT ON THE~~ INVESTIGATION OF BROAD-BAND EMITTERS AS POTENTIAL LASING IONS BETWEEN 0.5 AND 1.0 ~~μm~~ Micrometers.	5. TYPE OF REPORT & PERIOD COVERED: Interim Report 77 June 01-77 May 31
	6. PERFORMING ORG. REPORT NUMBER
7. AUTHOR(s): Charles F. Rapp, N. L. Boling, Cloyce M. Carlen	8. CONTRACT OR GRANT NUMBER(s): F44620-76-C-0088 new
9. PERFORMING ORGANIZATION NAME AND ADDRESS: Owens-Illinois, Inc. Corporate Technology P. O. Box 1035 Toledo, OH 43666	10. PROGRAM ELEMENT, PROJECT, TASK AREA & WORK UNIT NUMBERS: 61102F 2301/A1 A1
11. CONTROLLING OFFICE NAME AND ADDRESS: Director of Physics Air Force Office of Scientific Research Attn: NP Building 410, Bolling AFB, DC 20332	12. REPORT DATE: July 1977
	13. NUMBER OF PAGES: 58
14. MONITORING AGENCY NAME & ADDRESS (if different from Controlling Office): Interim rept. 1 Jun 76 - 31 May 77	15. SECURITY CLASS. (of this report)
	15a. DECLASSIFICATION/DOWNGRADING SCHEDULE

16. ~~DISTRIBUTION~~ STATEMENT (of this Report)

Approved for public release/distribution unlimited

64 p.

17. DISTRIBUTION STATEMENT (of the abstract entered in Block 20, if different from Report)

DDC AUG 22 1977 C

18. SUPPLEMENTARY NOTES

19. KEY WORDS (Continue on reverse side if necessary and identify by block number)

Glass Lasers, Tunable Lasers, Visible Lasers, Near IR Lasers, Broad-Band Fluorescence, Eu^{2+}, Cu^{+}, Sn^{2+}

20. ABSTRACT (Continue on reverse side if necessary and identify by block number)

Although fluorescent ions in glass were studied extensively during the 1960's for possible lasing action, these studies were primarily restricted to narrow emission band, long decay time ions such as the trivalent rare earths. This restriction was necessitated by the limited power of the then available flash-lamps. The development of powerful, short pulse flashlamps for dye layers in recent years has removed this constraint and now makes it feasible to consider broad-band emitters in glasses and crystals for lasing action. As opposed to the trivalent rare earths, which generally have their strongest fluorescent

over

DD FORM 1 JAN 73 1473 EDITION OF 1 NOV 65 IS OBSOLETE

Unclassified

SECURITY CLASSIFICATION OF THIS PAGE (When Data Entered)

408 243

LB

20. Abstract (continued)

lines in the near IR, broad-band emitters offer the possibility of visible and near UV lasers. Tuning over wide frequency ranges is also a possibility.

In this study, interest was primarily directed towards ions emitting in or near the spectral region between 0.5 μm and 1.0 μm.

A literature survey was done to identify any ions which might display a broad-band fluorescence in glass arising from an allowed electronic transition. A number of promising ions were identified which were either filled shell fluorescent ions or rare earths with broad emission bands. Glasses were prepared containing many of these ions and a spectroscopic evaluation was done for their lasing potential. Ions which appear most promising for lasing are the Eu^{2+}, Cu^{+}, and Sn^{2+} ions.

FOREWORD

Since June 1, 1976 we have been conducting a study of broad-band fluorescent ions in glass. This work has as its goal the assessment of the lasing potential of this until now largely unexplored class of ions. It is sponsored by the Air Force Office of Scientific Research under Contract F44629-76-C-0088. This contract was let in response to our July 1975 proposal entitled "An Investigation of Broad-Band Emitters as Potential Lasing Ions between 0.5 and 1.0 μm."

The 1975 proposal suggested a two-year program, the first year to be devoted to melting and spectroscopic studies of several ions in different glasses. During the second year actual lasing tests of the most promising ion-host combinations were to be conducted in conjunction with continued spectroscopic and melting work.

This report covers the work performed during the time period of the initial contract from June 1, 1976 to May 31, 1977. The materials preparation and spectroscopic evaluations called for under this contract are reported.

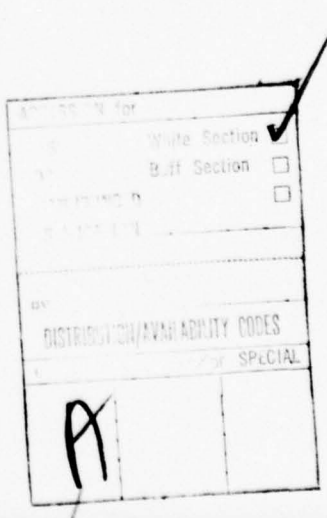

Abstract

Although fluorescent ions in glass were studied extensively during the 1960's for possible lasing action, these studies were primarily restricted to narrow emission band, long decay time ions such as the trivalent rare earths. This restriction was necessitated by the limited power of the then available flashlamps. The development of powerful, short pulse flashlamps for dye lasers in recent years has removed this constraint and now makes it feasible to consider broad-band emitters in glasses and crystals for lasing action. As opposed to the trivalent rare earths, which generally have their strongest fluorescent lines in the near IR, broad-band emitters offer the possibility of visible and near UV lasers. Tuning over wide frequency ranges is also a possibility.

In this study, interest was primarily directed towards ions emitting in or near the spectral region between 0.5 μm and 1.0 μm.

A literature survey was done to identify any ions which might display a broad-band fluorescence in glass arising from an allowed electronic transition. A number of promising ions were identified which were either filled shell fluorescent ions or rare earths with broad emission bands. Glasses were prepared containing many of these ions and a spectroscopic evaluation was done for their lasing potential. Ions which appear most promising for lasing are the Eu^{2+}, Cu^{+}, and Sn^{2+} ions.

Table of Contents

List of Tables

List of Figures

1. Introduction

Since the invention of the ruby laser in 1960, many fluorescent ions have been studied in regard to their lasing properties in glass or crystals. The peak activity in this work occurred in the early 1960's. Since a thorough investigation of a particular ion was an involved task, investigators had to choose carefully among the many candidate ions and host materials. In particular, the pumping power of available flashlamps had to be taken into account in deciding what ions to study. The pulses of these lamps were generally at least a few tens of microseconds in length, and this effectively limited the choice of ions in glass to the trivalent rare earths). Figure 1 shows the logic involved. The long pulses led to low temperatures and, therefore, to most efficient pumping in the visible and near IR where many RE^{3+} ions have strong absorption bands. The long pulse lengths also dictated long upper lasing level decay times and, consequently, low oscillator strengths. For sufficient cross section σ to achieve lasing, one could therefore consider only ions with narrow emission line-widths. This again led to RE^{3+} ions lasing in the near IR.

The result of these early investigations is synopsized in Table I where the ions presently known to lase in glass are listed. Some common features of these ions are:

1. All are trivalent rare earths (with narrow emission lines).
2. All emit in the near IR.
3. All are pumped in the visible and near IR.
4. All have long decay times (> 0.5 msec).

Recent developments in dye laser flashlamps have dramatically altered the necessity for the logic described above. A brief look at the history

of dye lasers illustrates the situation. It was first suggested in 1961 that dyes, because of their brilliant fluorescence, might make good laser materials. However, dyes are broad-band emitters with lifetimes of a few nanoseconds. They therefore require a very powerful pump source for lasing. Primarily as a consequence of this requirement, a dye laser was not realized until 1966 when a Q-switched ruby laser was used for pumping. A flashlamp-pumped dye, using a specially designed lamp, was made in the laboratory the next year. Powerful flashlamps for dye lasers became routinely available a few years afterward, and because of increasing interest in visible and near UV dye lasers, efforts to further improve these lamps are continuing.

Using these dye laser flashlamps developed since the activity peak in the search for new solid-state lasers, it becomes reasonable to reconsider broad-band, short lifetime emitters as lasing ions in glass. The logic of this is illustrated in Figure 2. Short ($\approx$ 1 μsec or less) pulses obtainable from dye lamps lead to high lamp temperatures and, therefore, to efficient UV pumping, so UV absorbers and near IR, visible or near UV emitters can be used. The short pulses also allow use of short lifetime ions with high oscillator strengths. These high oscillator strengths in turn result in a large σ even for broad-band emitters.

There are several broad-band ions that emit in the spectral range of interest to the Air Force (0.5 to 1.0 μm).[1] Those considered in this study fall into one of two classes: the rare earths with broad emission bands and filled shell fluorescent ions.

The broad ionic emission bands of interest here are associated with allowed transitions as opposed to the narrow emission bands associated with

forbidden transitions in the trivalent rare earth laser ions. It is desirable that these transitions be allowed so that their emission cross sections are large and their population inversions for threshold lasing are low, despite the large bandwidths. For the transitions to be allowed, the selection rule $\Delta\ell = \pm 1$ must be obeyed, and in surveying the various ions that fluoresce in glass, one finds that a relatively large number meet this criterion. In particular, Ce^{3+}, several of the divalent rare earth ions, and several filled shell fluorescent ions have allowed broad-band emission. However, in this study, interest is limited to these ions which emit in the spectral region of approximately 0.5 to 1.0 μm (that region of primary interest to the Air Force).[1]

2. Literature Survey

During the present contract, a literature survey was done in order to identify any fluorescent glasses that might be of interest to the Air Force. These glasses would be those which display a broad-band fluorescence arising from an allowed electronic transition in the region of 0.5 to 1.0 μm. Those ions which seemed to fall within the region of interest are given in Table II. Also listed in Table II are the electronic configurations of the ions, the approximately color of their fluorescence and several of the most pertinent references. Fluorescent glasses which were found but not included were those which contain ions displaying forbidden transitions (notably the trivalent rare earths, Mo^{3+} and Mn^{2+}) or which fluoresce at wavelengths significantly shorter than 5000 Å (for example, Tl^{+}, Pb^{2+}, and Ce^{3+}).

The 5,000 to 10,000 Å region of interest was not considered too rigidly since the absorption and emission processes taking place in the ions involve bonding orbitals and, therefore, very large changes in the spectral locations of the emission bands can take place when the chemical composition of the host is changed. These changes can be of the order of hundreds or even thousands of angstroms. This is quite apparent in the cases of Cu^{+} and Eu^{2+}.

This dependence of fluorescent wavelength on the host complicates the task of searching for ions to investigate for lasing in a particular spectral range. The task is further complicated by the broad band emission bands, since an ion with a peak fluorescence at, say, 4500 Å in a particular glass might be made to lase at 5500 Å, if the band is broad enough. On the other hand, these complexities are beneficial in that they yield more candidates for lasing in a particular region of interest.

For the ions listed, the number of references found varied from a great many for the case of the Cu^{+} ion to only one or two for the Ge^{2+}, Eu^{2+}, Yb^{2+}, and V^{5+} ions. Also, in the case of CdS, fluorescence in some glasses was reported but the activator was not identified.[1]

Generally, the literature search confirmed what we suspected on the basis of a cursory search done previous to work on this contract. That is, relatively little concerning fluorescence of most broad-band ions has been published; and as far as we can ascertain, hard data that would allow one to evaluate the lasing potential of any such ion do not exist.

3. Calculations Used for the Spectroscopic and Potential Lasing Evaluation

In order to roughly evaluate the lasing potential of a particular ion in a particular host, some ''guideline'' calculations are required. These calculations involve three steps:

a. Calculation of emission cross section σ.

b. Use of σ to calculate the population inversion ΔN required for threshold lasing.

c. Calculation of ΔN obtainable with a given pump source.

The stimulated emission cross section σ for a potential lasing transition from level 2 to level 1 can be calculated through the Füchtbauer-Landenburg equation:

$$\sigma = \frac{1}{\tau_{21}} \frac{\lambda^2}{8\pi\, n^2\, \Delta\nu} \qquad (1)$$

where λ is the line center frequency, $\Delta\nu$ is the line width, n is the index of refraction, and $1/\tau_{21}$ is the spontaneous transition rate from the upper lasing level to the lower level.

To use Eq. (1) it could be assumed that $\tau_{21} = \tau$, where τ is the measured fluorescent decay time or, more accurately, $\tau_{21} = \tau/\Phi$ where Φ is the quantum efficiency for the pertinent transition. The other parameters needed in Eq. (1) are obtained from the emission spectra.

Once σ is obtained, the population inversion ΔN required for threshold lasing is obtained straightforwardly from

$$r_1 r_2\, e^{2\ell(\sigma\Delta N - \alpha)} = 1 \qquad (2)$$

where r_1 and r_2 are mirror reflectivities, α is the loss per unit length, and ℓ is the rod length. To obtain representative numerical values for ΔN we choose

$r_2 = 1$

$r_1 = 0.95$

$\alpha = 0.01\ cm^{-1}$

$\ell = 3'' = 7.6\ cm$

Using these values in Eq. (2) gives

$$\Delta N = \frac{8.3 \times 10^{-3}}{\sigma}\ cm^{-3} \qquad (3)$$

After this calculation is done, one must then determine whether the threshold population inversions calculated can be achieved in order to estimate if lasing can be realized. To do this, the ionic absorption bands and the pump sources available must be taken into account. This calculation is done in some detail for several ions in a later section.

These calculations do not, of course, take into consideration the possibility of excited-state absorption. Since excited-state absorption can (and does) prevent lasing, the possibility of its existence cannot be ignored. However, since it is a much more difficult measurement to make, it is not a measurement considered here for screening materials, but one which is considered later with active lasing tests in the material evaluations.

4. Experimental Evaluation of Materials

On selected samples prepared with the various dopant ions, various spectroscopic measurements are made. These measurements include the fluorescent decay time, absorption spectra, emission spectra and quantum efficiency. From these measurements approximate laser thresholds for these materials can be calculated (as was discussed in the previous section).

Most of the above measurements are made by quite standard techniques. Since most ions of interest here have fluorescent decay times of a few microseconds or less, a Xenon Corporation Micropulser is used for the flash excitation. Generally, appropriate narrow band pass filters are used between the flashlamp and the sample and between the sample and the photomultiplier in order to block any stray excitation light from the detector.

Absorption spectra are taken with a Cary 14 Spectrophotometer. Emission spectra are recorded with a scanning quartz prism monochronometer in conjunction with a photomultiplier. (Generally an S-20 type; however, an S-1 type can be substituted to extend further into the IR.)

Quantum efficiency measurements are made by comparing the relative fluorescence output of the samples to a quinine sulfate -H_2SO_4 solution.

5. Experimental Results

Glasses Selected for Study

Of the dopant ions listed in Table I, glasses were prepared which contained the ions Cu^{+}, Ge^{2+}, Sn^{2+}, Sb^{3+}, Bi^{3+}, Eu^{2+}, and Yb^{2+}. Also, commercial filter glasses which contained CdS were obtained. The compositions of some select glasses prepared in the study are listed in Tables III and IV.

In a preliminary qualitative examination, the glasses containing Cu^{+}, Sn^{2+}, Sb^{3+}, and Eu^{2+} appeared to show the most promise without the need for more extensive development. Therefore, these ions have been the most thoroughly investigated thus far. However, several of the other glasses have shown very interesting features and promise and should be investigated as time permits.

In the following discussion the ions which have been investigated the least but which appear to be very interesting for future investigation will be discussed first.

5.1. Ge^{2+} Doped Glasses

Glasses doped with Ge^{2+} can be produced by strongly reducing glasses containing GeO_2. This was accomplished in this study in the same manner as described elsewhere;[4] that is, by the addition of some glass constituents as acetates and melting in a covered SiO_2 crucible. Ge^{2+} was easily produced in the Na_2O-CaO-SiO_2 glass (AF-117) but, as reported elsewhere,[4] no Ge^{2+} was produced in the K_2O-BaO-GeO_2 glass without NiO (AF-127) but was in the glass containing a trace of NiO (AF-128). This is a puzzling but interesting phenomenon that deserves further investigation.

The production of Ge^{2+} could easily be detected visually by the yellow color imparted to the glass. Also, the red fluorescence from the Ge^{2+} could

easily be seen when the glass was exposed to ''long wave'' UV excitation. However, because of the uncertainty in how much GeO_2 was reduced, it was very difficult to estimate the amount of Ge^{2+} produced.

The Ge^{2+} ion is one of the ions that appears very interesting for further study since it has a fluorescence that peaks well into the red and since it has a very broad absorption band in the blue (see Figure 3) which should result in very efficient pumping.

5.2. CdS Containing Glasses

Cadmium sulfide containing glasses can be made to absorb and emit throughout quite a large range in the visible and near-infrared, depending on their composition and the melting and heat-treatment conditions. Therefore, these glasses could be of considerable interest here.

In this study, rather than expend a considerable effort on the development of preparation techniques for these glasses, commercially available filter glasses were purchased. These glasses show considerable fluorescence under UV excitation but have not yet been evaluated spectroscopically. That is, the absorption, emission and excitation spectra, quantum efficiency, and decay times have not yet been measured.

5.3. Yb^{2+} Doped Glasses

Several attempts were made to generate Yb^{2+} in Vycor, as was described by Wachtel.[10] However, this ion appeared to be quite difficult to generate. When using ytterbium nitrate to impregnate the Vycor, substantial amounts of Yb^{2+} could only be produced when the Vycor was also impregnated with large amounts of aluminum nitrate (as was reported by Wachtel). However, when a solution of ytterbium acetate was used to impregnate the ''thirsty Vycor,''

and the sample fired in a 100% H_2 atmosphere, substantial amounts of Yb^{2+} could be generated without the addition of the extra aluminum salts.

Figures 4 and 5 show the absorption and emission spectra of Yb^{2+} doped Vycor produced by impregnating ''thirsty Vycor'' with a solution of ytterbium acetate. (While the amount of reduction of the ytterbium has not yet been quantitatively determined, this sample would contain 0.10 weight % YbO if all the ytterbium were reduced.) As can be seen, the emission peaks at about 5500 Å and extends out past 7000 Å. This is in about the ideal region for this study. However, most of the intense absorption of the Yb^{2+} is in the UV with a somewhat weak tail extending into the visible. This tail is apparently responsible for the excitation spectra (as shown by Wachtel) extending out to about 4500 Å.

The fluorescence decay time of this glass was found to be 52 μsec. Also, the quantum efficiency was found to be about 7.2% under 2537 Å excitation (see Table V). Using these two values, a radiative decay time for the Yb^{2+} could be calculated to be 720 μsec. This decay time is extremely long and would be indicative of a forbidden transition. This transition may be the same as that which is responsible for the very weak absorption seen between 3000 and 5000 Å. In order to calculate what fluorescent decay time would be expected for this transition, it would be necessary to know both the amount of Yb^{2+} generated and the nature (the multiplicity) of the ground and the excited states of the observed absorption. However, from the intensity of the absorption observed at about 3500 Å, a fluorescent decay time of several hundred microseconds would not be unreasonable.

The reason for the relatively long fluorescent decay time of the Yb^{2+} ion is not immediately obvious. It would be expected that the emission would

be from an allowed d → f transition, similar to the Eu^{2+} ion. However, this does not appear to be the case. It can only be speculated at this time but it may be that the strong UV absorption (< 3000 Å) is due to an allowed f → d transition. However, if a p orbital lies at a slightly lower energy than the upper d orbital, a decay from the d to the p orbital could take place producing a forbidden p → f emission to the ground state.

In order to determine whether the Yb^{2+} ion still has potential as a broad band laser ion, it will be necessary to determine the significance of the low quantum efficiency. That is, if the excited state responsible for the fluorescence is actually being quenched by some mechanism so that the radiative decay time is about 700 μsec (as calculated from τ/Φ), then the stimulated emission cross section for the Yb^{2+} ion would probably be too low to expect lasing to occur at a reasonable threshold. However, if the quantum efficiency is low because of some other mechanism, such as only a partial decay into this energy level, then the quantum efficiency from the fluorescent state itself may be nearer to 1.0 and the radiative decay time of this state may be near the measured 50 μsec. This radiative decay time would then give an emission cross section which would be reasonable to expect lasing. In order to distinguish between these possibilities, it will be necessary to measure the quantum efficiency of the fluorescent level. This might be done by direct excitation into the lower lying energy level with 3500 Å radiation as opposed to the 2537 Å radiation used previously.

5.4. Eu^{2+} Doped Glasses

The absorption and emission spectra of Eu^{2+} in various silicate glasses have been given elsewhere,[1] but in order to generate Eu^{2+} in those glasses

it was necessary to melt the glasses in graphite crucibles which reduced the glasses so severely that the glasses were somewhat darkened and showed considerable light scattering. Therefore, in order to obtain good optical-quality samples for the present study, Eu^{2+} doped Vycor was produced as described by Wachtel.[10] Since Eu^{2+} can be generated much more easily in "high silica" glasses (such as Vycor or fused silica) than it can be in more conventional silicate glasses, almost all the europium doped into Vycor can be reduced to the Eu^{2+} state under quite mildly reducing conditions (10% H_2-90% N_2 atmosphere). (As a matter of fact, the blue Eu^{2+} fluorescence could be seen even in a sample which had been fired in air. It would be interesting to establish the $Eu^{2+} \rightleftharpoons Eu^{3+}$ equilibrium in this material as a function of the oxygen partial pressure.)

Figures 6, 7, and 8 show the absorption spectra, emission spectra, and the "photon emission spectra" of an Eu^{2+} doped "96% silica" glass containing approximately 0.02 wt % EuO. As can be seen from the figures, this ion should be easily pumped with a flashlamp because of its broad absorption band.

Unfortunately, Eu^{2+} emission in this "96% silica" host is at somewhat shorter wavelengths than is desired for Air Force applications. However, since Eu^{2+} emission in other glass hosts is at considerably longer wavelengths, it may be possible to shift the emission in the "96% silica" host by impregnating "thirsty Vycor" with another ion at the same time it is impregnated with the europium salts. We have attempted to do this with aluminum nitrate and phosphoric acid, but the concentrations were apparently too high and the samples crumbled in firing. Further attempts at shifting the Eu^{2+} emission are planned.

By integrating the area under the emission curve shown in Figure 8, and by comparing this to a similar emission curve obtained for quinine sulfate, and correcting for the amount of light absorbed by both samples at 2537 Å, it was found that the quantum efficiency of the Eu^{2+} fluorescence was 0.77. This quantum yield is very high and is therefore very encouraging for laser applications.

The fluorescent decay time of this sample, under flash excitation at about 2540 Å, was found to be 1.9 μsec (see Table V). If this value is corrected by the quantum efficiency (assuming the decrease in the quantum efficiency below 1.0 is due to nonradiative decay from the excited state) the radiative decay time for the Eu^{2+} ion is 2.5 μsec.

5.5. Cu^{+} Doped Glasses

A series of Cu^{+} doped glasses (see Table III) was prepared by melting the glasses in a gas-fired pot furnace with an excess of CH_4 (with respect to air) to produce a reducing atmosphere. This was quite effective in reducing all the copper as no blue color (Cu^{2+}) was evident in the glasses. However, some light scatter could be seen in the sample indicating the glasses may have been too strongly reduced.

The absorption spectra, emission spectra, and "photon emission spectra" of the two glasses containing 0.05 mole % Cu_2O are shown in Figures 9 through 15. The light scattering mentioned previously is apparent in the absorption spectra shown in Figures 9 and 10. That is, it appears that there is an absorption tail extending throughout most of the visible. Actually, the Cu^{+} absorption in this glass should approach zero near 350 nm as does the spectrum shown in Figure 13 for the Na_2O-CaO-SiO_2 glass.

The areas obtained from the emission curves shown in Figures 12 and 15 were used to calculate the quantum efficiencies of the fluorescence when the samples were excited at 2537 Å. It was found that the quantum efficiency of the Cu^+ fluorescence in the Li_2O-CaO-SiO_2 glass (AF-110) was 0.61 and the quantum efficiency of the Cu^+ fluorescence in the Na_2O-CaO-SiO_2 glass (AF-104) was 0.67. Also, the fluorescent decay times of these glasses were found to be 32.4 μsec for the Li_2O-CaO-SiO_2 glass (AF-110) and 27.2 for the Na_2O-CaO-SiO_2 glass (AF-104). Using the measured quantum efficiencies to correct these values, radiative decay times are 53 μsec for AF-110 and 41 μsec for AF-104.

5.6. Sn^{2+} Doped Glasses

A series of Sn^{2+} doped glasses (see Table III) was prepared. The absorption and emission spectra of some of these glasses are shown in Figures 16 through 22. Under 2537 Å excitation the quantum efficiency for the silicate glasses was found to vary between 0.12 and 0.47. The reason for this variation in quantum efficiencies becomes apparent when examining the absorption spectra of these glasses, and the undoped base glass, shown in Figure 16. That is, the absorption by the base glass is quite intense at 2537 Å (1.30 cm^{-1}) and can effectively compete for the absorption of light with the Sn^{2+} ion in the more lightly doped glasses. For example, the absorption intensities are about 1.85 cm^{-1} and 5.78 cm^{-1} at 2537 Å for the doped glasses containing 0.01 and 0.1 mole % SnO. Using these values and that of the undoped glass, the measured quantum efficiencies of the Sn^{2+} fluorescence can be corrected, giving 0.40 and 0.44 (as compared to 0.47 measured for the 1.0 mole % SnO glass). Using these values and the measured

fluorescent decay times (when excited at about 2540 Å and measured through a Schott BG18 green filter glass transmitting greater than 40% from ≈ 3500 Å to 6000 Å) radiative decay rates of about 41 μsec are obtained (see Table V).

As might be expected from the appearance of the Sn^{2+} emission spectra, the emission from these glasses appears white. This seems very desirable for the ''tunable'' laser application since any wavelength throughout the visible might be selected. However, the band at 400 nm and the band at 600 nm apparently arise from two different initial energy levels. That is, in a previous unpublished work it was found that the 400 nm emission band is quite strong when the glass is excited at about 2500 Å but nearly disappears from the emission spectrum when the glass is excited at longer UV wavelengths. Although some estimate is made in Section 6 as to the Sn^{2+} potential for lasing, more spectroscopic work should be done to determine more accurately the quantum efficiencies, fluorescent decay times, and excitation spectra for the two bands. However, even with this complication, the estimate made of the emission cross section of the Sn^{2+} ion is probably not greatly in error.

It is possible that the same phenomenon is being observed in the Sn^{2+} ion in silicate glasses as is taking place in the Cu^{+} ion. That is, the absorption is taking place in an allowed transition with short wave excitation. Direct emission from this level would be in the 400 nm band which may have a short decay time. However, most of the energy may decay to a slightly lower lying level which then has a forbidden transition and therefore a relatively long decay time. The 600 nm band would then result from the forbidden transition. The present data are not sufficient to establish this but it is hoped that these measurements can be made.

The fluorescent decay time for Sn^{2+} was found to be considerably shorter in a phosphate glass than the silicate glass. The quantum efficiency was also found to be about 22%. However, since an undoped sample of the phosphate glass was not prepared, any possible interference by the base glass absorption in the quantum efficiency measurement was not determined. Therefore, the calculated radiative decay time of 26 μsec is probably a maximum and may be considerably shorter. From this it might be concluded that the fluorescent decay time of the Sn^{2+} ion is <u>at least</u> two times shorter in the phosphate glass than in the silicate glasses with a correspondingly greater emission cross section. Therefore, the Sn^{2+} ion in phosphate glass may be a very promising laser species.

6. Calculations of Lasing Potential

Using the spectroscopic data presented in Section 5 we can roughly appraise the lasing potential of Eu^{2+} in Vycor (fused quartz), Cu^{+} in Na_2O-CaO-SiO_2 and Li_2O-CaO-SiO_2 glasses, and Sn^{2+} in Na_2O-SiO_2 glasses. To do these approximatations we follow the procedure discussed in our 1975 proposal. That is, we use spectroscopic data to calculate the stimulated emission cross section σ and then assume practical laser cavity and rod parameters to calculate the population inversion required for threshold lasing. An estimation of the population inversion achievable is made by considering flashlamp parameters and coupling of flashlamp energy into the rod. Comparison of the required and attainable inversion energies then yields the desired estimation of lasing potential.

Results of calculations for the four cases are summarized in Tables VI and VII. Details of the calculations are as follows:

6.1. Eu^{2+} in Vycor

The Füchtbauer-Ladenburg equation is used to calculate σ:

$$\sigma = \frac{1}{\tau_{21}} \frac{\lambda^2}{8\pi n^2 \Delta\nu} \quad , \tag{1}$$

where $1/\tau_{21}$ is the spontaneous transition rate from the upper to the lower lasing level, λ is the center wavelength of the emission line, $\Delta\nu$ is the width of the emission line, and n is the refractive index.

We obtain τ_{21}, λ, and $\Delta\nu$ from the data of Section 5 (Figure 7).

$\tau_{21} = \tau/\phi = 2.5 \times 10^{-6}$ sec ($\tau = 1.9$ μsec and $\phi = 0.77$)

$\lambda = 4.2 \times 10^{-5}$ cm

$\Delta\nu = 1.1 \times 10^{14}$ sec^{-1}

Taking n = 1.46 then yields, from Eq. (1), $\sigma = 1.1 \times 10^{-19}$ cm^2.

We proceed now to calculation of the population inversion ΔN required for threshold lasing. Given the stimulated emission cross section σ, ΔN is obtained from

$$r_1 r_2 \, e^{2\ell(\sigma \Delta N - \alpha)} = 1 \quad , \tag{2}$$

where r_1 and r_2 are mirror reflectivities, ℓ is the rod length, and α is the loss per unit length. We choose

$r_2 = 1$

$r_1 = 0.95$

$\alpha = 0.01$ cm^{-1}

$\ell = 3'' = 7.6$ cm

to obtain

$$\Delta N = \frac{8.3 \times 10^{-3}}{\sigma} \text{ cm}^{-3} \quad . \tag{3}$$

Using the calculated value of σ we get $\Delta N = 6.8 \times 10^{16}$ cm^{-3} for threshold lasing.

It will be convenient to convert this required threshold population inversion to a required threshold energy absorption for the whole rod. To do this we choose a rod diameter of 0.3 cm (rod volume = 0.54 cm^3). Taking the average energy required to excite one ion as that associated with the center of the useful absorption band ($\approx$ 2800 Å in this case, from Figure 6), and assuming that every excited ion eventually decays to the upper lasing level, we find that the rod must absorb 0.027 J to achieve threshold lasing.

It now remains only to estimate the energy available for absorption by the rod. From Figure 6 we find the useful pump band for a 0.3 cm rod. (This is done by simply multiplying the absorbance/cm shown in the figure by 0.3, thus yielding a new absorbance curve for a 0.3 cm rod.) Taking the short wavelength pump limit to be that corresponding to an absorbance of 2.0 in a distance of 3 mm we find the pump limit to be approximately 2200 Å. However, at 2200 Å the host absorbance in 3 mm is 1.4. This implies that an unacceptable 70% of the pump energy at 2200 Å is absorbed by the host rather than the dopant ion. Therefore we take the pump limit to be only 2300 Å, where the host absorbance is negligible compared to that of the dopant.

(This illustrates an important problem, not only for Eu^{2+} but also for other broad-band ions discussed in this proposal. It is desirable to keep the host absorption edge far enough into the UV so that the high absorbance of the dopant ion rather than of the host dictates the short wavelength pump limit. This is made all the more important by the rise of the flashlamp emission spectrum toward shorter wavelengths.)

The long wavelength pump limit is obtained by requiring 30% absorption in 3 mm. From Figure 6 this limit is found to be 3600 Å.

To find the flashlamp energy within this 2300-3600 Å pump band, we use the same estimations as in our 1975 proposal, leading to 25 J of light energy from a 25,000°K lamp operating at a pulse length significantly shorter than the Eu^{2+} decay time of 1.9 μsec. From the 25,000°K black-body curve for such a lamp we find that about 18% of this 25 J, or 4.5 J, is emitted in the 2300-3600 Å interval. Assuming a rod-lamp coupling coefficient of 0.5, we finally obtain 2.3 J absorbed by the laser rod in the useful pump band.

This attainable 2.3 J is to be compared to the 0.027 J required for threshold lasing. Thus, barring phenomena such as unexpectedly high excited state absorption, Eu^{2+} in Vycor should be a very good lasing material.

6.2. Cu^{+} in Na_2O-CaO-SiO_2 Glass

Proceeding as for Eu^{2+} we find from the data of Section 5 (Figures 13 and 14)

$$\lambda = 5.1 \times 10^{-5} \text{ cm}$$

$$\Delta\nu = 1.9 \times 10^{14} \text{ sec}^{-1}$$

$$\tau_{21} = 4 \times 10^{-5} \text{ sec } (\tau = 27 \text{ sec}, \varphi = 0.67)$$

$$n = 1.5$$

These data yield $\sigma = 6.0 \times 10^{-21}$ cm^2 and ΔN for threshold lasing = 1.4×10^{18}/cm^3. The associated required absorbed energy, taking the weighted center of the useful absorption band at 2500 Å, is 0.6 J for a 3'' x 3 mm rod.

Because of the relatively long decay time of Cu^{+}, a longer flashlamp pulse can be used. We take this lamp pulse length to be 10-15 μsec. (This is enough shorter than the Cu^{+} decay time of 27 μsec so that negligible energy is lost due to spontaneous emission during the lamp pulse.) This longer pulse leads to a cooler lamp temperature, which we estimate to be 15,000°K. From the 15,000°K black-body curve, approximately 17% of the lamp emission lies in the useful pump band of 2350-2400 Å (Figure 13).

From data on commercially available linear flashlamps, we find that approximately 48 J of light can be obtained from two linear lamps operating at one half their explosion energy. Thus 0.17 x 48 = 8.2 J is emitted from the lamp within the useful band. Again using a rod-lamp coupling coefficient of 0.5, we obtain 4.1 J absorbed by the rod within the useful pump band.

This 4.1 J is to be compared to the 0.6 J required for threshold lasing.

6.3. Cu^{+} in Li_2O-CaO-SiO_2 Glass

Again proceeding as for Eu^{2+} we find (Figures 9 and 11)

$\lambda = 4.8 \times 10^{-5}$ cm

$\Delta\nu = 1.46 \times 10^{14}$ sec^{-1}

$\tau_{21} = 5.4 \times 10^{-5}$ sec (τ = 32 μsec, Φ = 0.61)

n = 1.5

This gives $\sigma = 3.9 \times 10^{-21}$ cm^2, ΔN for threshold lasing = $2.1 \times 10^{-18}/cm^3$, and required absorbed energy = 0.9 J.

The pump band and lamp parameters are taken to be the same as those for the Cu^{+} in Na_2O-CaO-SiO_2 discussed in 6.2, yielding an available absorbed energy of 4.1 J. Thus the required and available absorbed energies for this glass are 0.9 J and 4.1 J, respectively, leading one to conclude that Cu^{+} in an Na_2O-CaO-SiO_2 glass is preferable to Cu^{+} in an Li_2O-CaO-SiO_2 glass for lasing tests. The longer emission wavelength of the Na glass is also preferable for Air Force applications, although the emission band broadness of the Li glass would probably also yield lasing at greater than 5000 Å.

6.4. Sn^{2+} in Na_2O-SiO_2 Glass

Again proceeding as for Eu^{2+} we find (Figures 16 and 17)

$\lambda = 5.5 \times 10^{-5}$ cm

$\Delta\nu = 4.2 \times 10^{14}$ sec^{-1}

$\tau_{21} = 0.40 \times 10^{-4}$ sec (τ = 19.0 μsec, Φ = 0.47)

n = 1.5

This gives $\sigma = 3.1 \times 10^{-21}$ cm^2 and ΔN for threshold lasing = $2.7 \times 10^{18}/cm^3$.

Taking the weighted center of the useful pump band to be at 2600 Å, the absorbed energy required at threshold is 0.9 J for the 3'' x 3 mm rod.

Using Figure 16 to obtain the absorbance for a 3 mm path length, we find the short wavelength pump limit to be about 2100 Å for a properly chosen dopant concentration (the lowest concentration shown in Figure 16). However, at 2100 Å the host absorbance is 1.3 for a 3 mm sample. We are required therefore to select the next highest dopant concentration of Figure 16, which leads to a pump limit of 2400 Å where the host absorbance is nearly negligible compared to the dopant absorbance.

For a 15,000°K lamp, which we will use for this calculation, approximately 10% of the black-body radiation lies between 2400 and 2800 Å, while about 20% lies between 2100 and 2800 Å. The available pump energy is therefore severely limited by host absorption in this case.

Using the same lamp and coupling parameters as for Cu^{+}, an absorbed energy of 2.4 J is obtained. This is compared with 0.9 J required for threshold lasing, leading one to infer that Sn^{2+} in a silicate glass is a promising lasing ion. Even more promising, however, is the Sn^{2+} doped phosphate glass which may require only about 0.2 to 0.5 J for threshold.

References

1. Unsolicited Research Proposal Submitted to the Air Force Office of Scientific Research, ''An Investigation of Broad-Band Emitters as Potential Lasing Ions Between 0.5 and 1.0 μm,'' July 1975.

2. K. Patek, Glass Lasers, CRC Press, Cleveland, OH (1970).

3. S. Parke and R. S. Webb, ''Fluorescence of copper in glass,'' Phys. and Chem. of Glasses, 13 (6) 157-160 (1972).

4. C. Hirayama and F. E. Camp, ''Fluorescence of Fe, Co, and Ni in Reduced Germanate Glass,'' J. Electrochem. Soc., 115 (12) 1275-1279 (1968).

5. S. Parke and R. S. Webb, ''Optical properties of Sn^{2+} and Sb^{3+} in calcium metaphosphate glass,'' J. Phys. D:Appl. Phys., Vol. 4, 825-828 (1971).

6. Richard Stephen Webb, ''The optical properties of filled-shell ions in glass,'' Doctor of Philosophy thesis, University of Sheffield, 1969.

7. W. A. Weyl, Colored Glasses, reprinted by Dawson's of Pall-Mall, London (1959), p. 492.

8. C. S. French, ''Fluorescence spectra of sharp cut-off filters,'' Appl. Optics, 4 (4) 514 (1965).

9. Loren N. Pfeiffer and John F. Porter, Jr., ''Fluorescence of red glass filters,'' Appl. Optics, 3 (2) 317 (1964).

10. A. Wachtel, ''Divalent rare earth activated 96% SiO_2 glass,'' J. Electrochem. Soc., 117 (5) 708-711 (1970).

11. S. Parke and R. S. Webb, ''The optical properties of thallium, lead and bismuth in oxide glasses,'' J. Phys. Chem. Solids, 34, 85-95 (1973).

12. J. H. Mackey and J. Nahum, ''Spectral study of the interconversion of Eu^{2+} and Eu^{3+} in silicate glasses,'' Phys. and Chem. of Glasses, 9 (2) 52-63 (1968).

Table I

Ions Presently Known to Lase in Glass and Their Common Features

	λ (μ)	τ (msec)
Yb^{3+}	1.015	1.5
Nd^{3+}	1.06	0.5
Er^{3+}	1.54	15.0
Tm^{3+}	1.85	0.5
Ho^{3+}	2.08	0.8

Common Features of All:

1. Are trivalent rare earths
2. All emit in near IR
3. Are pumped in visible and IR
4. Have long decay times ($\geq$ 0.5 msec)

Table II

Dopants in Glass which Fluoresce at Wavelengths Greater Than 5000 Å

Ion	Configuration	Fluorescence color	Reference
Cu^{+}	d^{10}	blue-green	3, 6
Ge^{2+}	s^2	orange-red	4
Sn^{2+}	s^2	white	5, 6
Sb^{3+}	s^2	whitish-blue	5, 6
Bi^{3+}	s^2	blue (narrow red?)	6, 11
V^{5+}	rare gas	yellow	7
CdS	molecule	variable thru vis. and IR	8, 9
Eu^{2+}	rare earth	blue to green	1, 2, 10
Yb^{2+}	rare earth	green	10

Table III

Compositions of Select Glasses
Melted for Spectroscopic Studies

	AF-103	AF-104	AF-105	AF-109	AF-110	AF-111
SiO_2	73.51	73.51	73.51	60.0	60.0	60.0
Al_2O_3	1.00	1.00	1.00	2.5	2.5	2.5
Li_2O	--	--	--	27.5	27.5	27.5
Na_2O	13.13	13.13	13.13	--	--	--
CaO	12.36	12.36	12.36	10.0	10.0	10.0
Cu_2O	--	0.05	0.01	--	0.05	0.01
Atm:	Excess CH_4 in gas-air fired furnace →					

	AF-117	AF-118	AF-119	AF-120	AF-121	AF-122
SiO_2	50.0	75.0	75.0	75.0	75.0	75.0
Na_2O	22.0	25.0	25.0	25.0	25.0	25.0
CaO	8.0	--	--	--	--	--
GeO_2	20.0	--	--	--	--	--
SnO	--	--	0.01	0.1	1.0	--
Sb_2O_3	--	--	--	--	--	0.1
Atm:	sodium added as acetate - melted in covered crucible	air in electric furnace →				

	AF-123	AF-124	AF-125	AF-126	AF-127	AF-128
CaO	50.0	50.0	50.0	--	--	--
P_2O_5	50.0	50.0	50.0	--	--	--
K_2O	--	--	--	17.0	17.0	17.0
BaO	--	--	--	17.0	17.0	17.0
GeO_2	--	--	--	66.0	66.0	66.0
SnO	0.1	--	--	--	--	--
Sb_2O_3	--	0.1	--	--	--	--
Bi_2O_3	--	--	0.1	--	--	--
NiO	--	--	--	--	--	0.01
Atm:	air →			made from carbonate constituents	K and Ba added as acetates - melted in covered crucible	

Table IV

Compositions of Vycor Doped Samples
Prepared for Spectroscopic Studies

	7414-8G*		7414-114A**	
SiO_2	96.3	(by difference)		Nominally the same as 7414-8G. However, was not analyzed and was a different lot of Vycor.
Na_2O	0.025	chemical analysis of commercial Vycor (96% SiO_2)		
Al_2O_3	0.32			
B_2O_3	3.34			
Fe_2O_3	0.004			
EuO	0.02		--	
YbO	--		0.10	
Atm:	fused in 10% H_2 - 90% N_2		fused in 100% H_2	

* Prepared by soaking porous Vycor in a solution containing 0.00187 g of $Eu(NO_3)_3 \cdot 6H_2O$ per cc of solution. Concentration was chosen so that absorbance would be about 4/cm at peak of Eu^{2+} absorption according to data of J. H. Macky and J. Nahum.

** Prepared by soaking porous Vycor in a solution containing 0.0037 g Yb_2O_3 per cc of solution as ytterbium acetate.

Table V

Fluorescent Decay Time and
Quantum Efficiencies of Select Glasses

	Host	Ion	τ (μsec)	ϕ	ϕ^*	τ_{21} (μsec)
7414-8G	Vycor	Eu^{2+}	1.9	0.77	--	2.5
7414-114A	Vycor	Yb^{2+}	52.0	0.072	--	720
AF-119	Na_2O-SiO_2	Sn^{2+}	16.3	0.12	0.40	41
AF-120	Na_2O-SiO_2	Sn^{2+}	19.1	0.34	0.44	43
AF-121	Na_2O-SiO_2	Sn^{2+}	19.0	0.47	0.47	40
AF-123	CaO-P_2O_5	Sn^{2+}	5.8	0.22	--	26
AF-110	Li_2O-CaO-SiO_2	Cu^{+}	32.4	0.61	--	53
AF-111	Li_2O-CaO-SiO_2	Cu^{+}	33.1	--	--	
AF-104	Na_2O-CaO-SiO_2	Cu^{+}	27.2	0.67	--	41
AF-105	Na_2O-CaO-SiO_2	Cu^{+}	29.4	--	--	
AF-122	Na_2O-SiO_2	Sb^{3+}	9.6			

τ = measured fluorescent decay time

ϕ = quantum efficiencies

ϕ^* = quantum efficiencies corrected for interference by base glass absorption

τ_{21} = radiative decay time

Table VI

Data Used in Obtaining Stimulated Emission Cross Sections σ and Resulting Values of σ for the Four Glasses of Section 6

	Eu^{2+}	Cu^{+} in Na Glass	Cu^{+} in Li Glass	Sn^{2+}
τ (10^{-6} sec)	1.9	27	32	19
ϕ	0.77	0.67	0.61	0.47
τ_{21} ($= \tau/\phi$)(10^{-6} sec)	2.5	41	53	40
λ (Å)	4200	5100	4800	5500
$\Delta\lambda$ (Å)	700	1600	1500	3700
$\Delta\nu$ (10^{14} sec^{-1})	1.1	1.9	1.96	4.2
σ (10^{20} cm^2)	11	0.60	0.39	0.31

τ = fluorescent decay time

ϕ = quantum efficiency

τ_{21} = radiative decay time upper to lower level

λ = wavelength of emission band center

$\Delta\lambda$ = FWHM of emission band

$\Delta\nu$ = FWHM of emission band

σ = stimulated emission cross section

Table VII

Results of Lasing Threshold Calculation for Four Glasses of Section 6

A 3'' x 3 mm laser rod, mirror reflectivities of 100% and 95%, and a loss coefficient of 0.01 cm^{-1} are assumed. Lamp and other parameters are as discussed in Section 6 and our 1975 proposal.

	Eu^{2+}	Cu^{+} in Na Glass	Cu^{+} in Li Glass	Sn^{2+}
ΔN (10^{18} ions/cc)	0.068	1.4	3.9	2.7
$\Delta\lambda\|_{pump}$ (Å)	2300-3600	2350-2900	2350-2900	2400-2800
E_A (J)	0.024	0.59	0.89	0.90
E_A' (J)	2.3	4.1	4.1	2.4

ΔN = ion population inversion required at threshold

$\Delta\lambda\|_{pump}$ = useful pump band

E_A = required absorbed energy at threshold

E_A' = actual energy absorbed

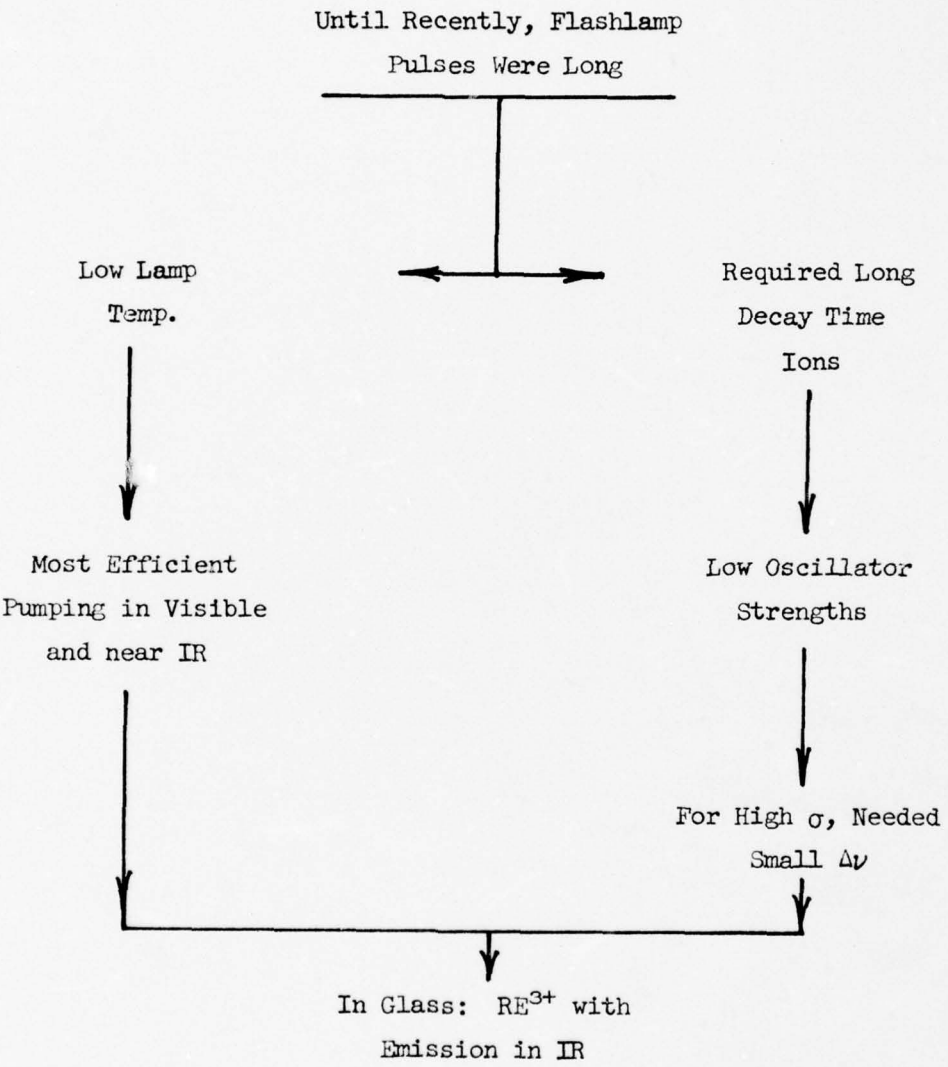

Figure 1 - Logic Dictated by Long Pulse (a few tens of μsec) Flashlamps

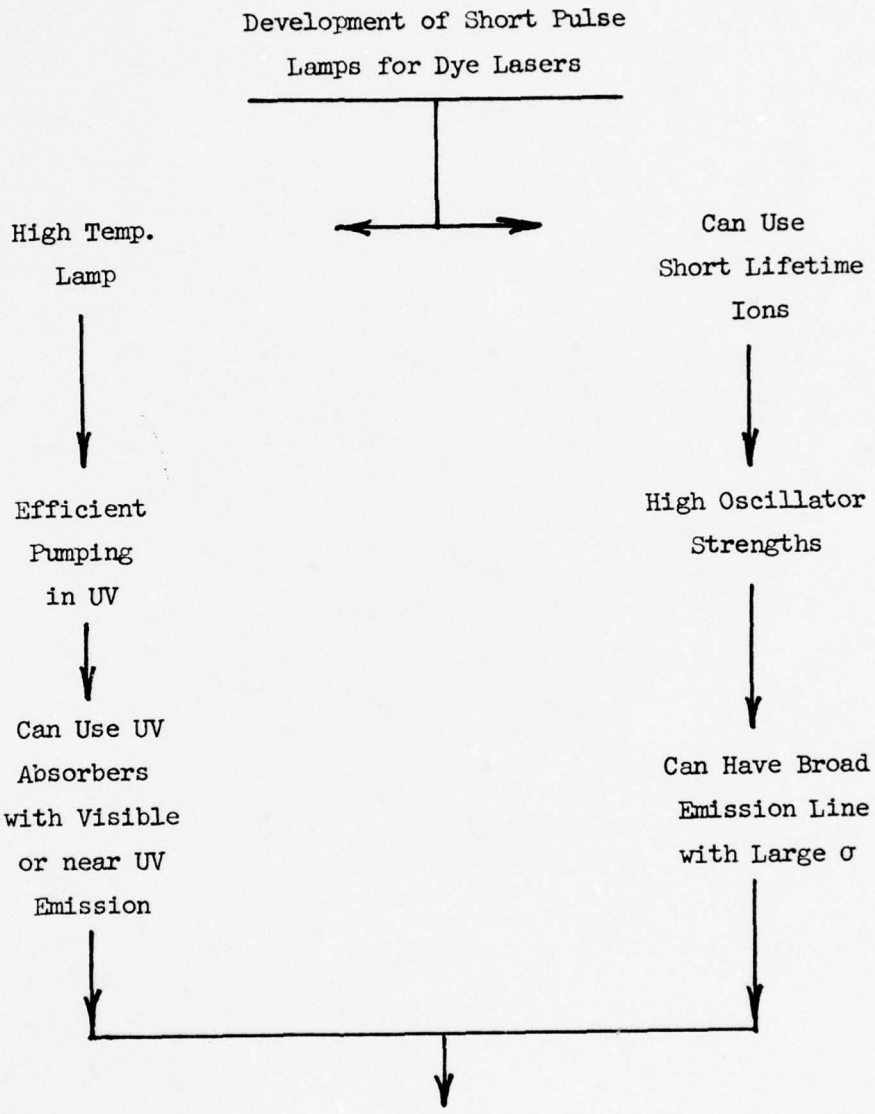

Figure 2 - Logic Allowed by Use of Short Pulse (μsec, or less) Dye Laser Flashlamps

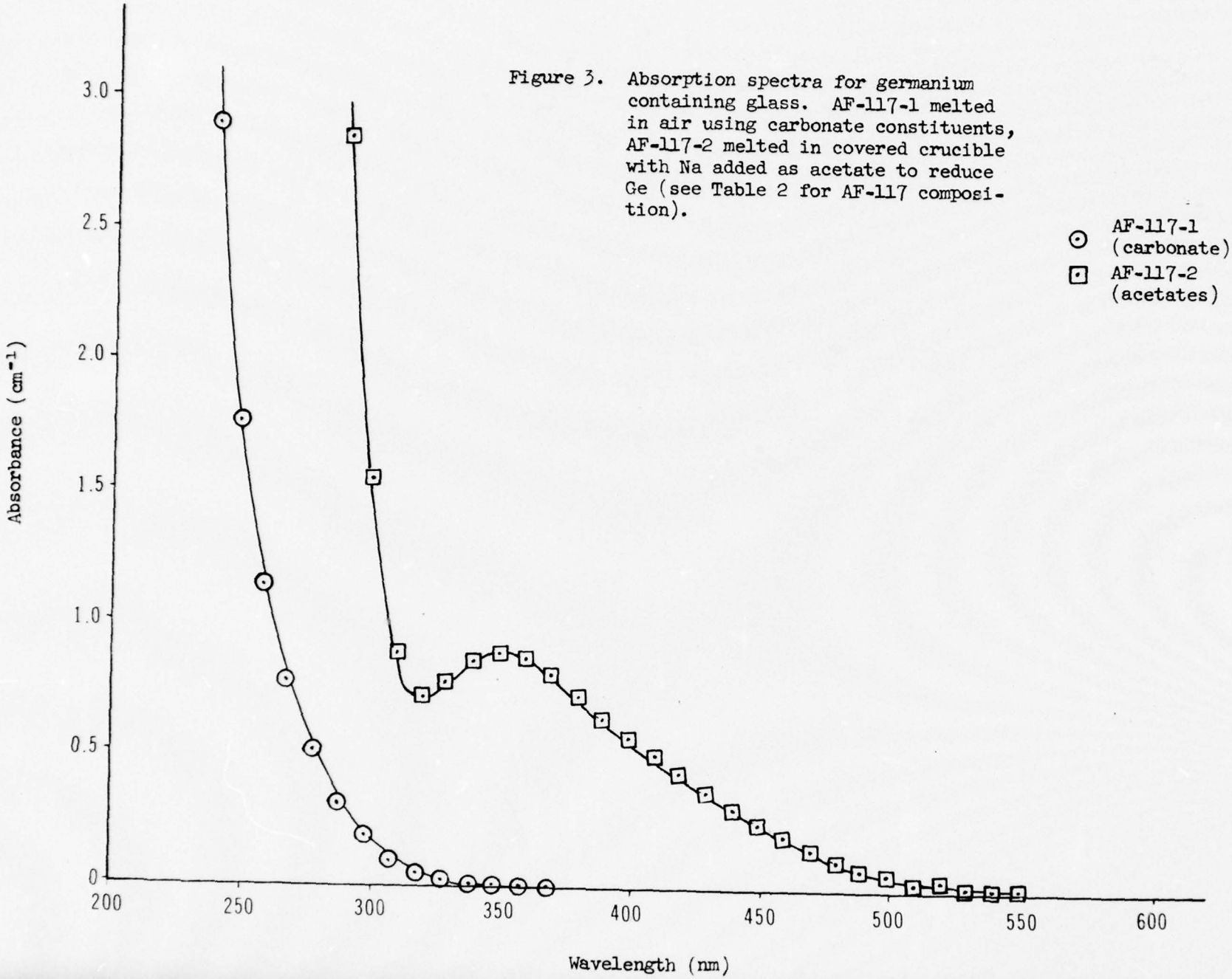

Figure 3. Absorption spectra for germanium containing glass. AF-117-1 melted in air using carbonate constituents, AF-117-2 melted in covered crucible with Na added as acetate to reduce Ge (see Table 2 for AF-117 composition).

Figure 4. Absorption Spectra for Sintered Vycor and Yb^{2+} Doped Vycor

Sample 114A [YbO] ≈ 0.1 wt %

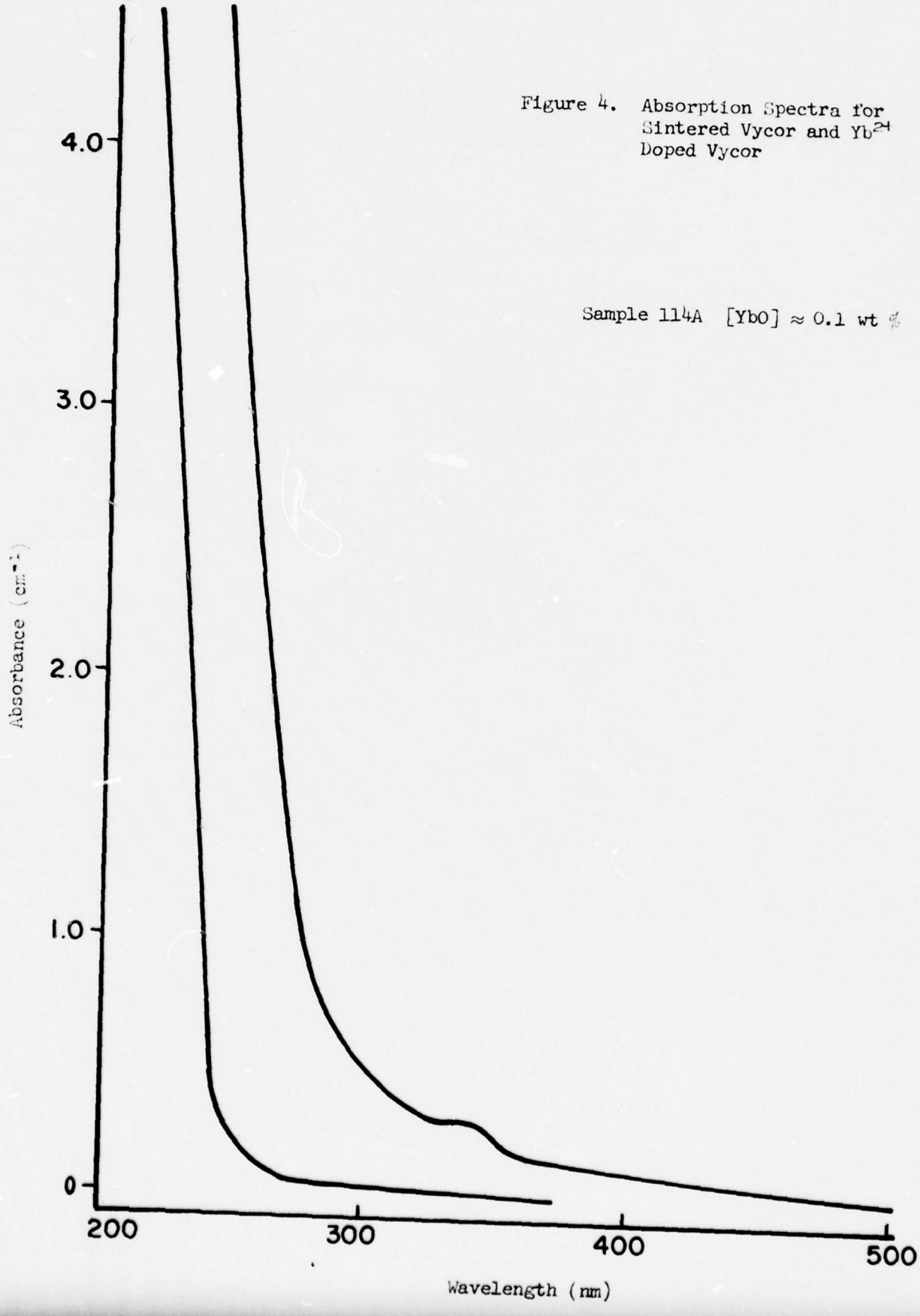

Figure 5. Emission Spectra of Yb^{2+} Doped Vycor

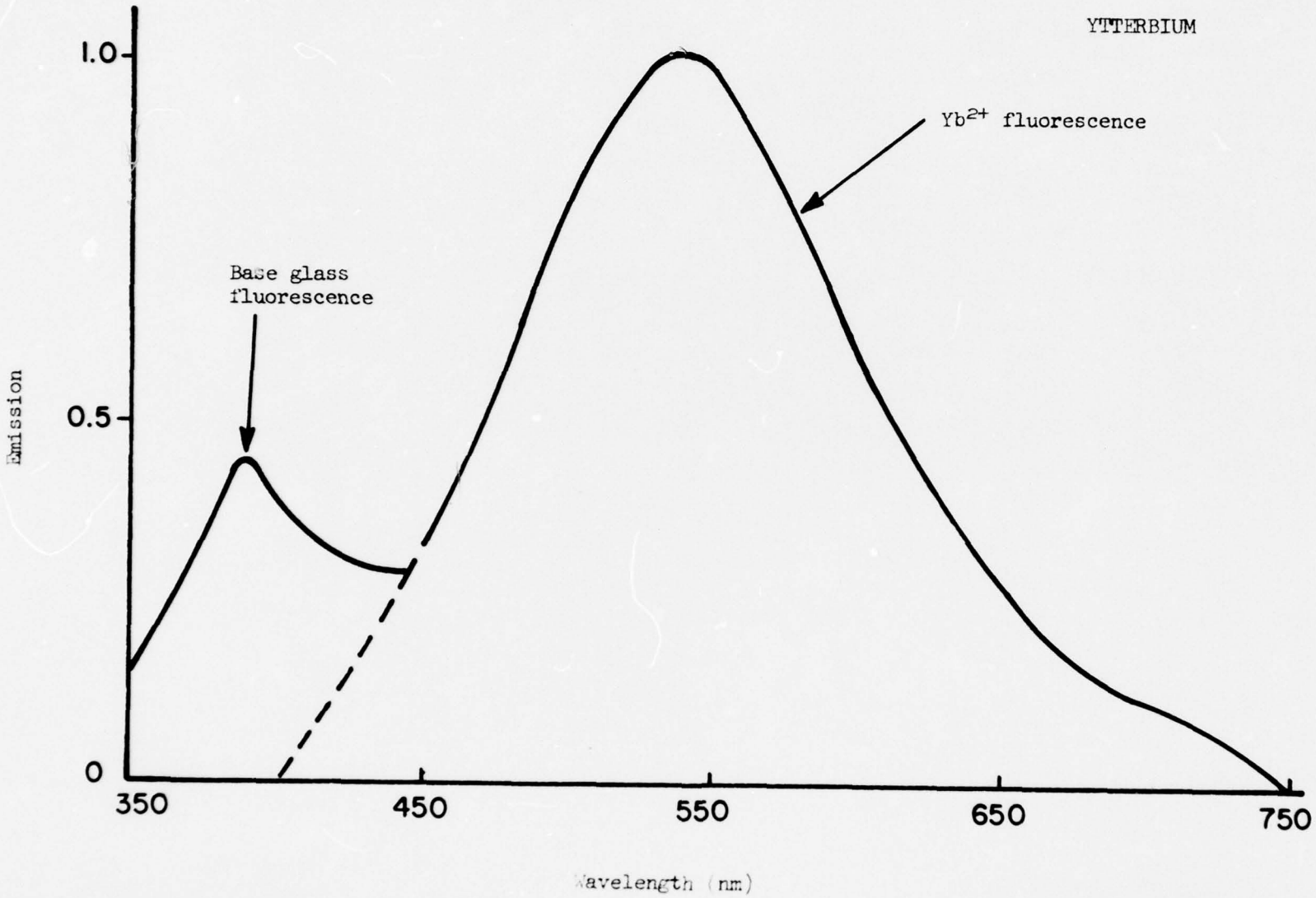

Figure 6. Absorption spectra for sintered Vycor and europium doped Vycor fused in a 10% H_2-90% N_2 atmosphere. For composition see glass 7414-8G in Table 2.

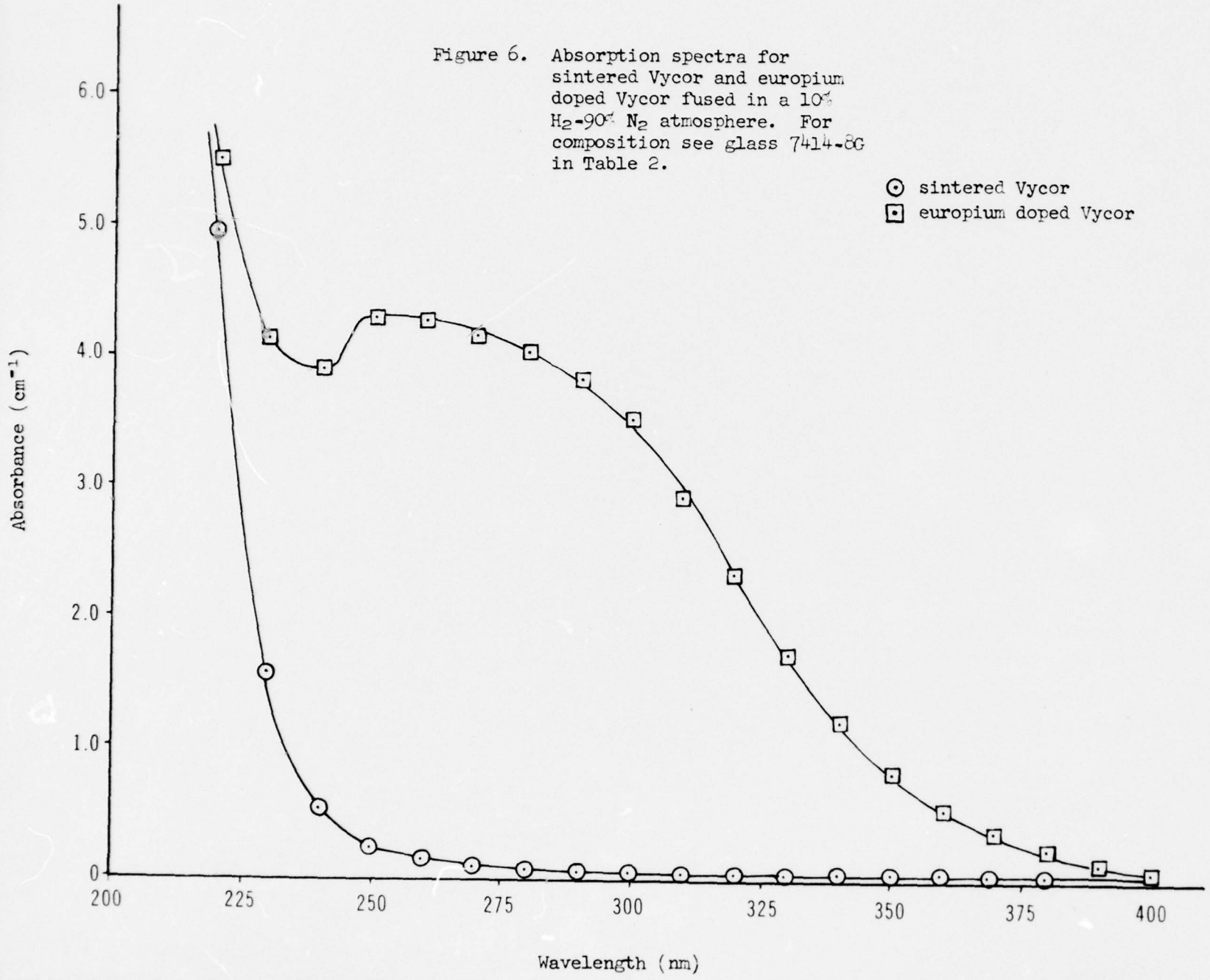

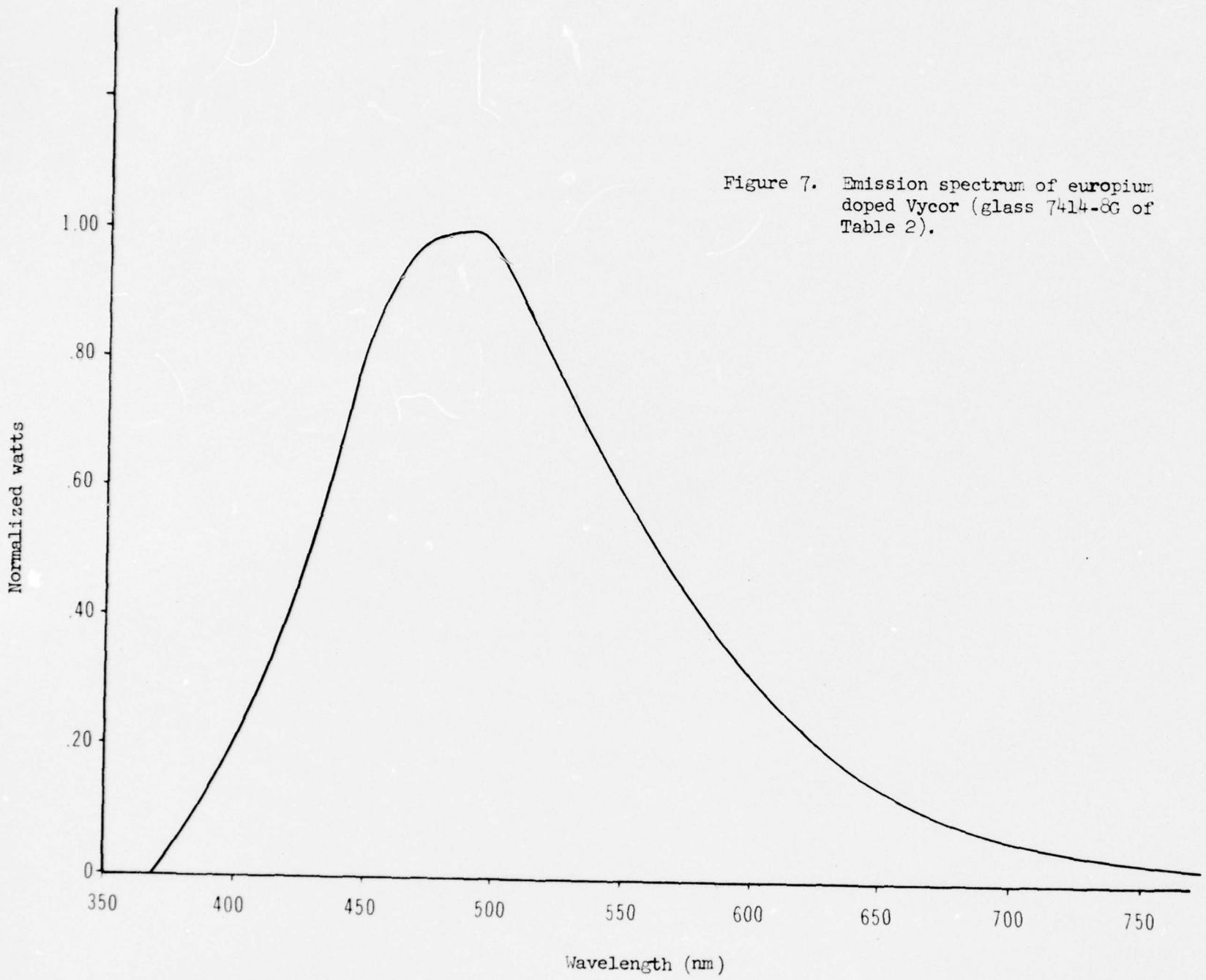

Figure 7. Emission spectrum of europium doped Vycor (glass 7414-8G of Table 2).

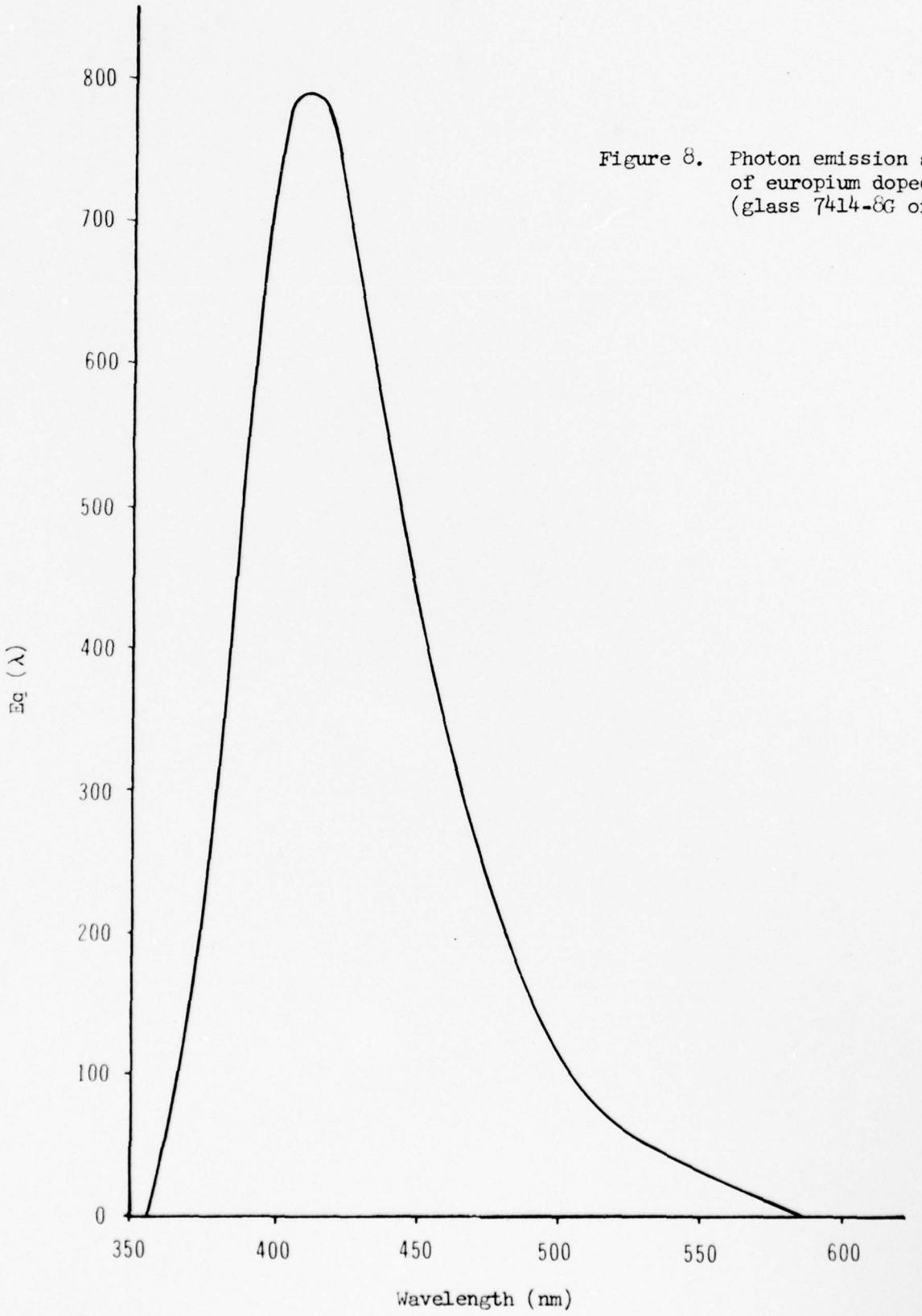

Figure 8. Photon emission spectrum of europium doped Vycor (glass 7414-8G of Table 2)

Figure 9. Absorption spectra of undoped and Cu^+ doped Li_2O-CaO-SiO_2 glasses (see glasses AF-109 and AF-110 of Table 2 for compositions)

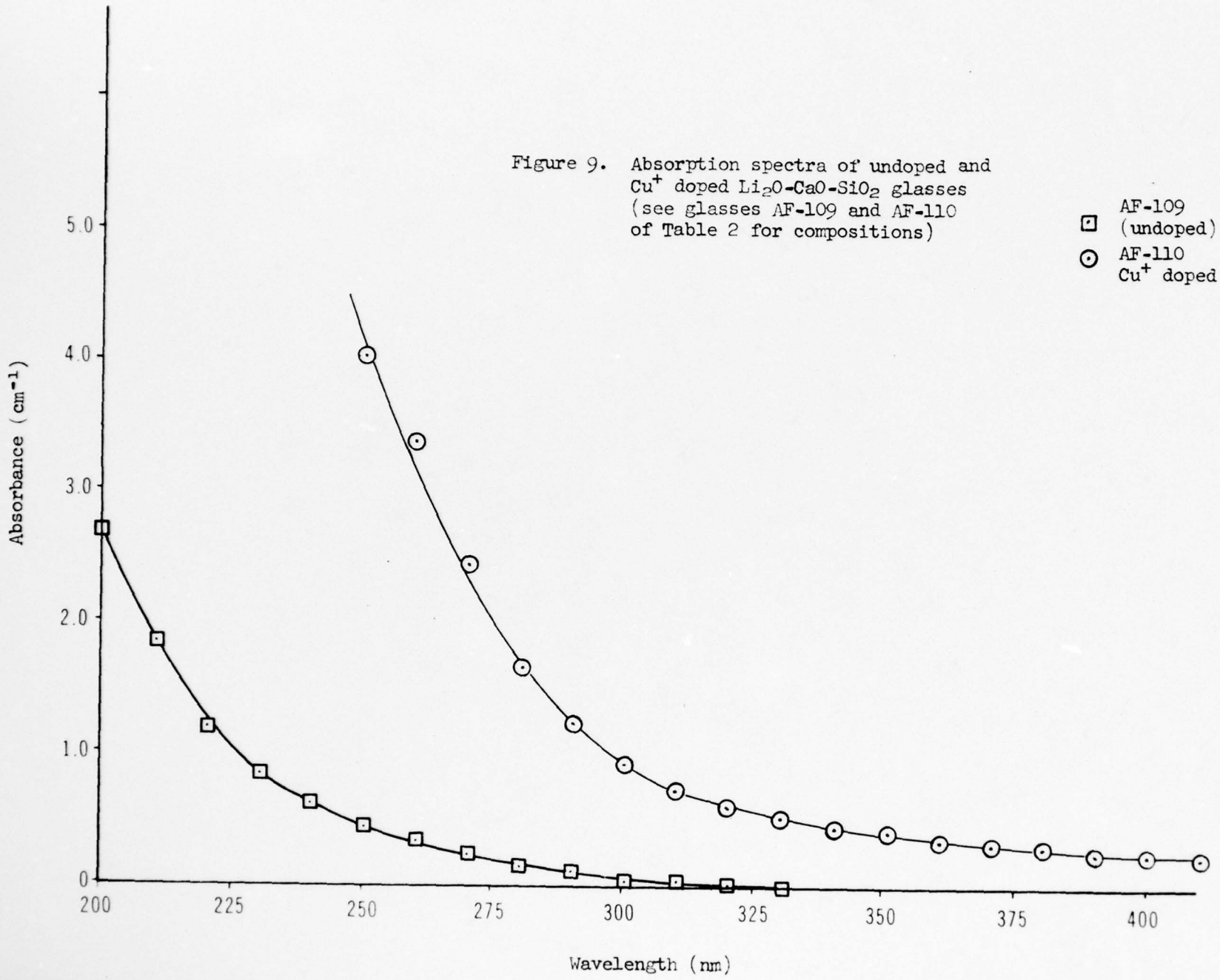

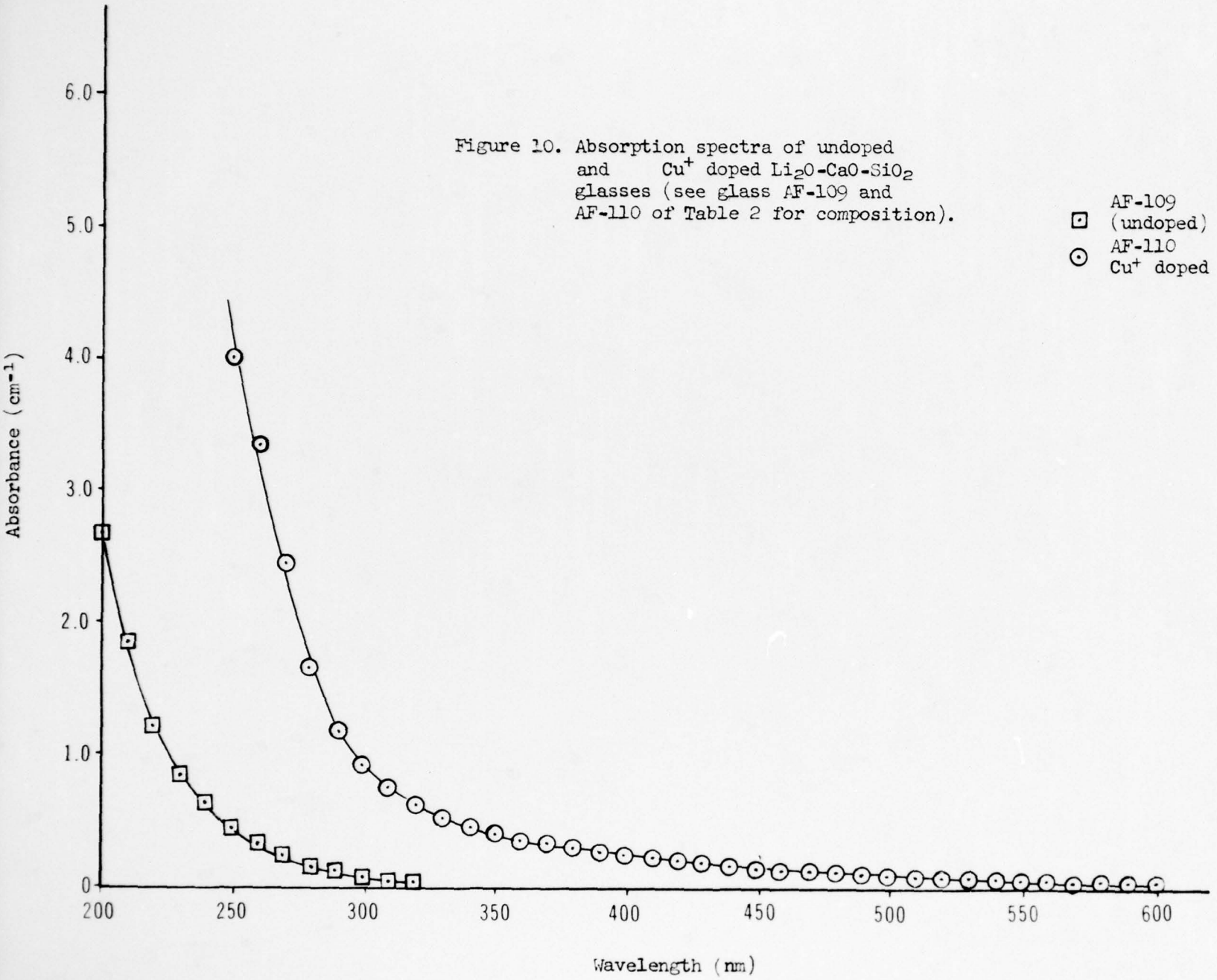

Figure 10. Absorption spectra of undoped and Cu^{+} doped Li_2O-CaO-SiO_2 glasses (see glass AF-109 and AF-110 of Table 2 for composition).

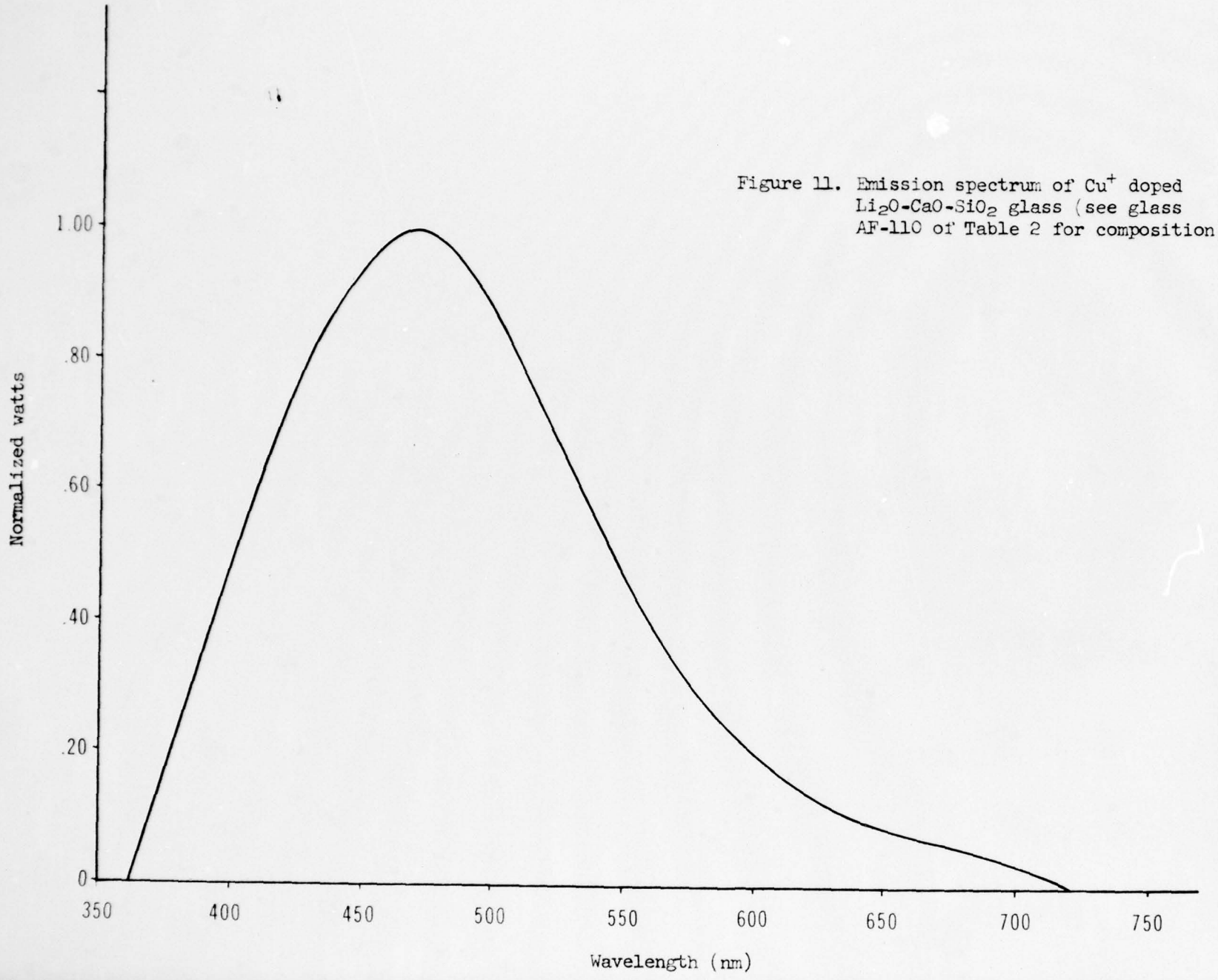

Figure 11. Emission spectrum of Cu^{+} doped Li_2O-CaO-SiO_2 glass (see glass AF-110 of Table 2 for composition).

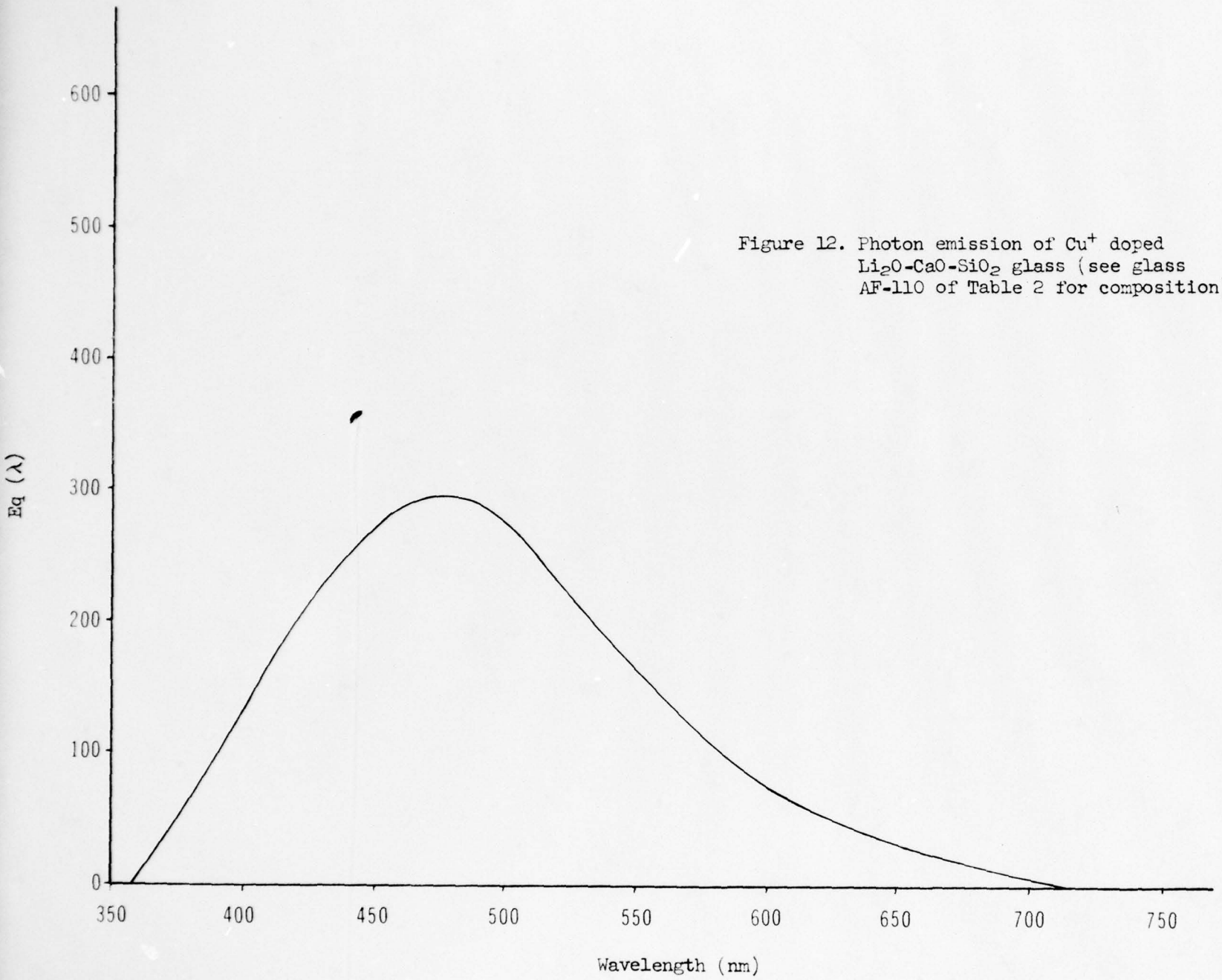

Figure 12. Photon emission of Cu^{+} doped Li_2O-CaO-SiO_2 glass (see glass AF-110 of Table 2 for composition).

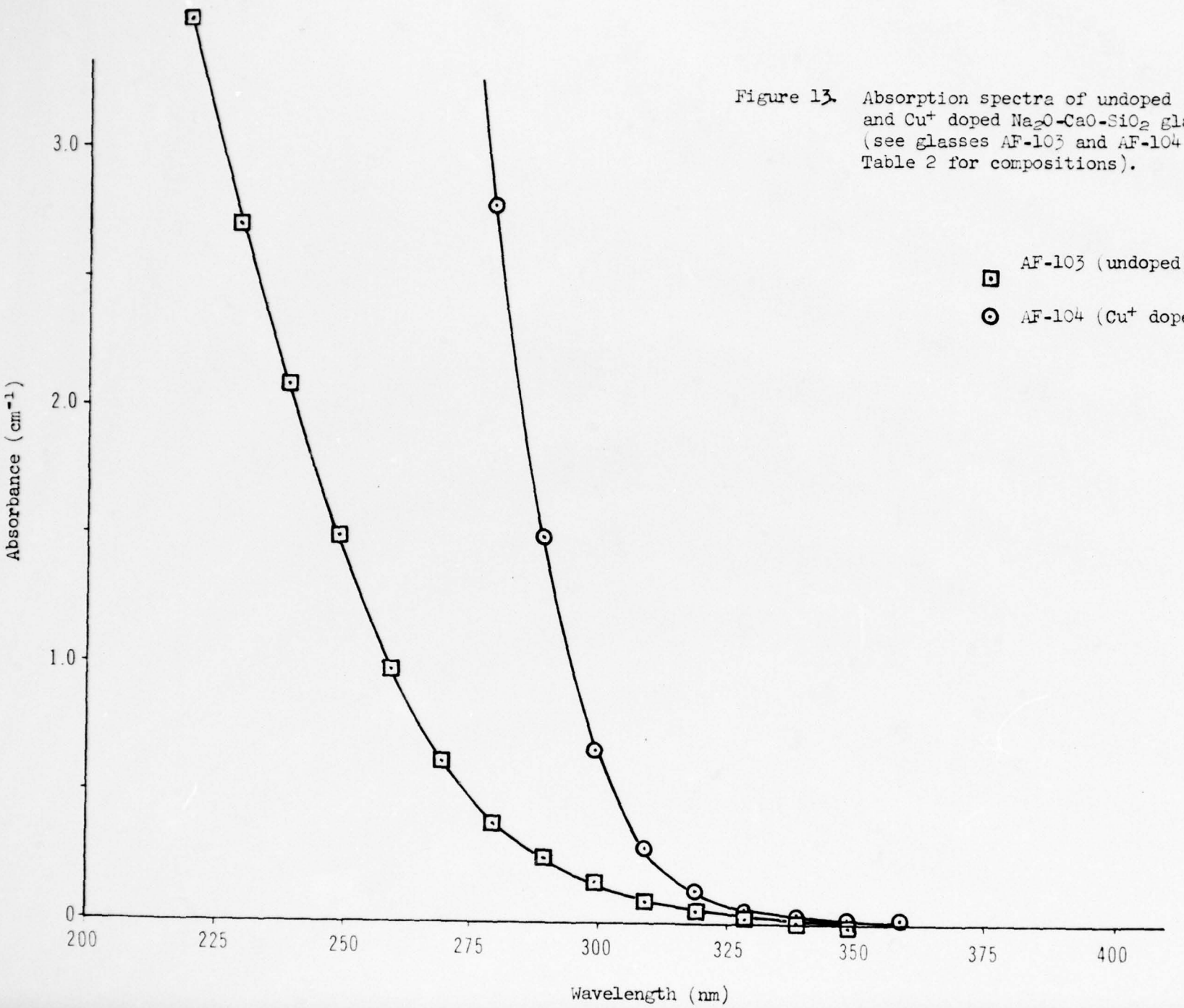

Figure 13. Absorption spectra of undoped and Cu^+ doped Na_2O-CaO-SiO_2 glasses (see glasses AF-103 and AF-104 of Table 2 for compositions).

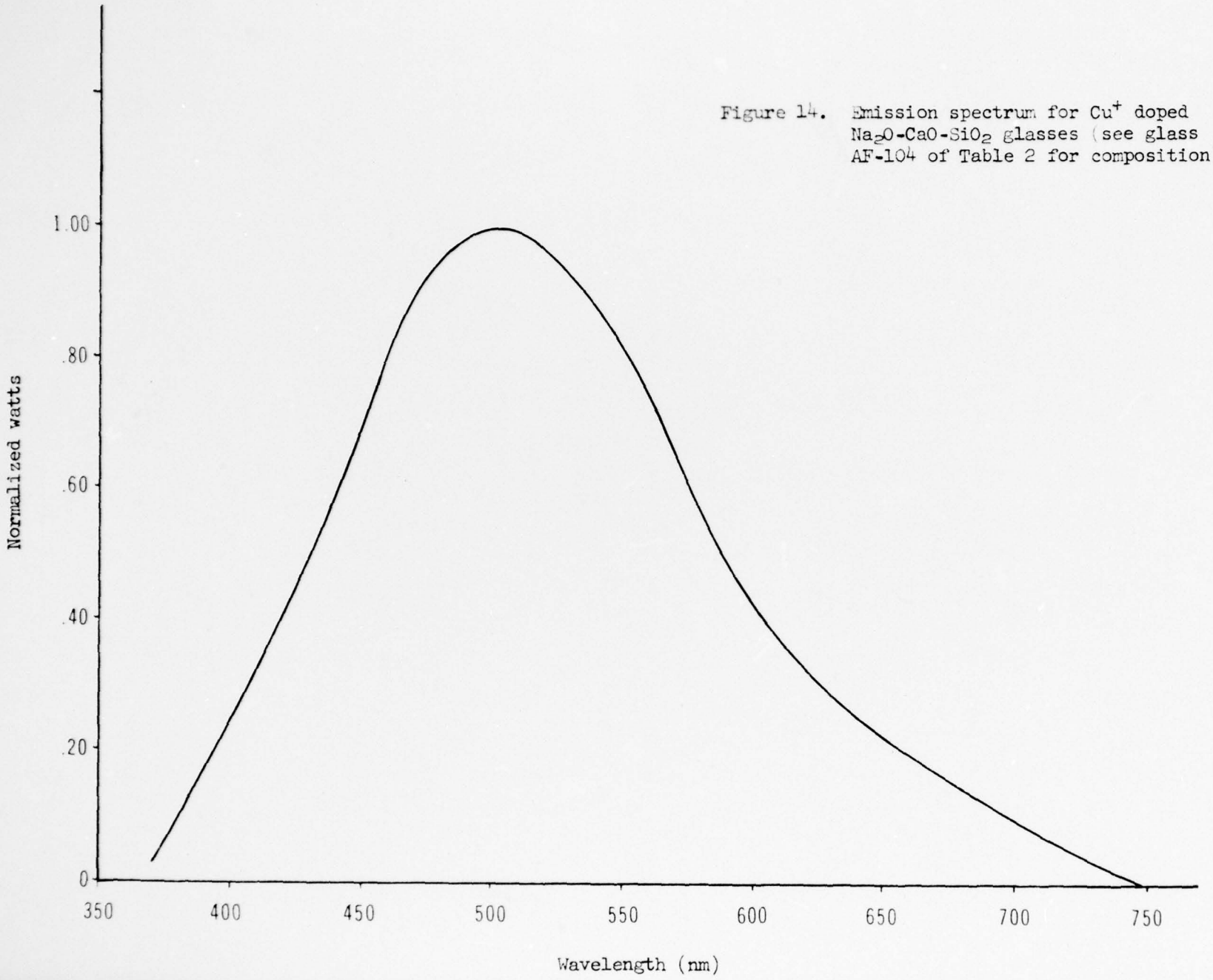

Figure 14. Emission spectrum for Cu^{+} doped Na_2O-CaO-SiO_2 glasses (see glass AF-104 of Table 2 for composition).

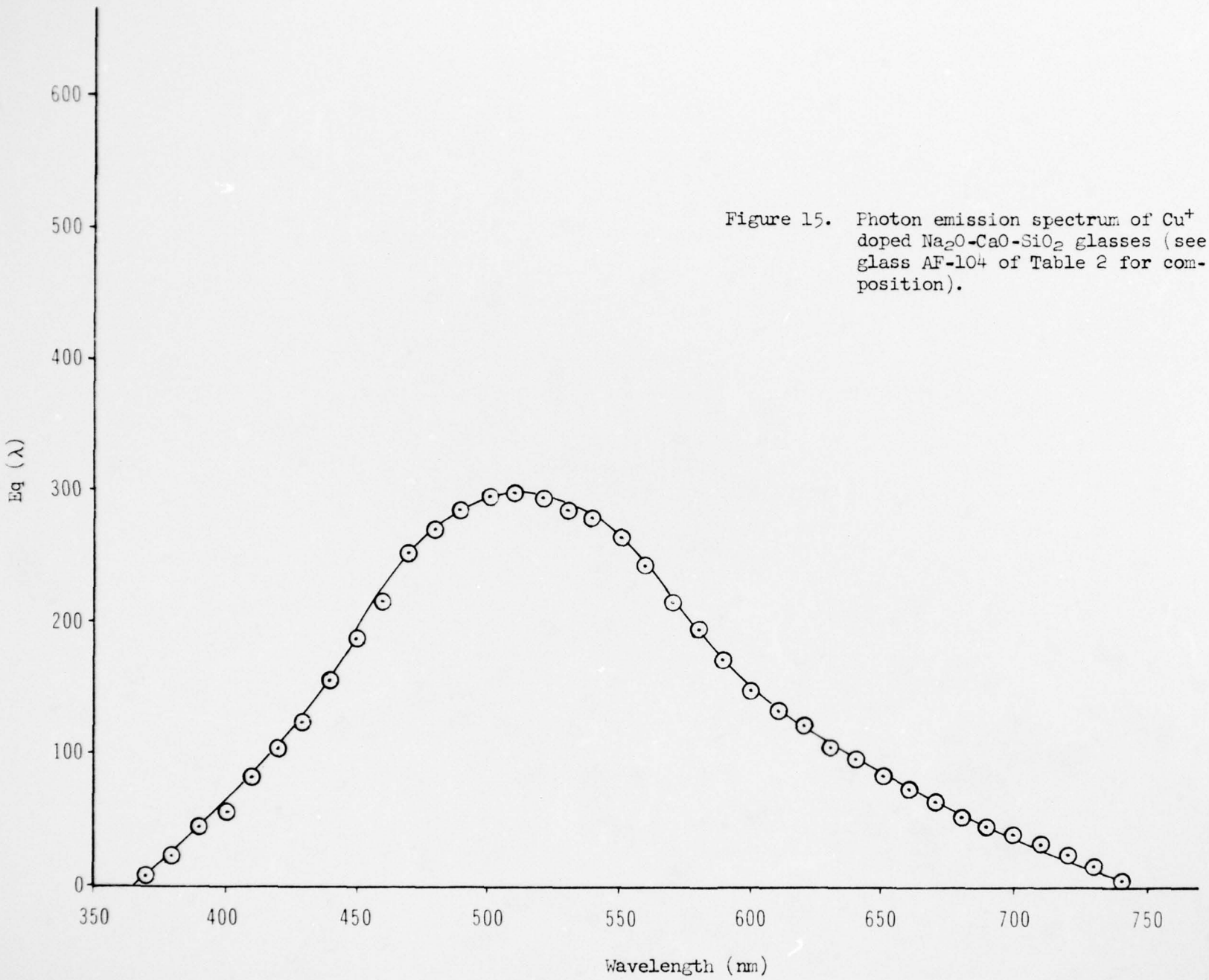

Figure 15. Photon emission spectrum of Cu^{+} doped Na_2O-CaO-SiO_2 glasses (see glass AF-104 of Table 2 for composition).

Figure 16. Absorption spectra of undoped and Sn^{2+} doped Na_2O-SiO_2 glasses, with various concentrations of Sn. (see glasses AF-118, AF-119, AF-120, and AF-121 of Table 2 for compositions).

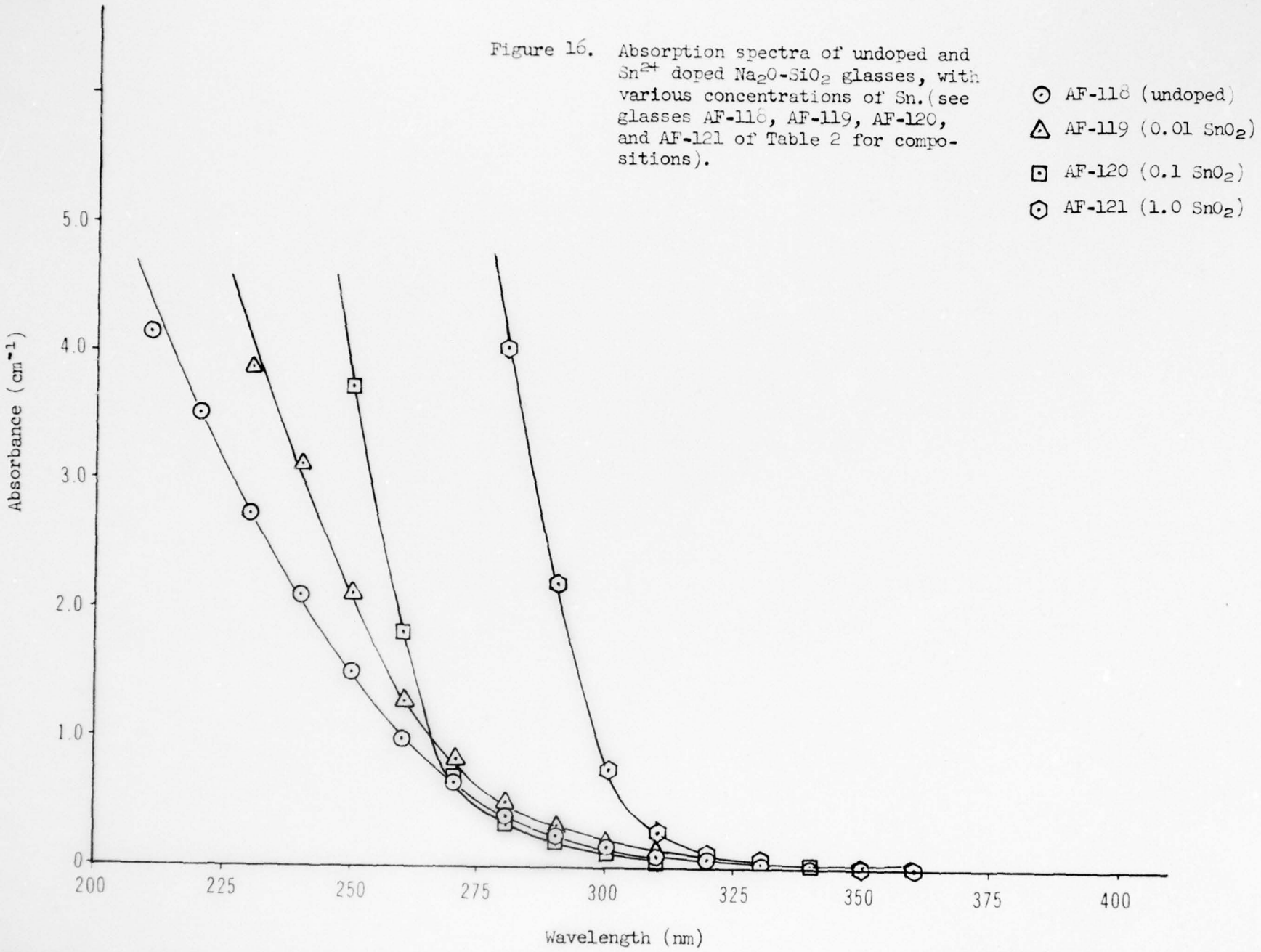

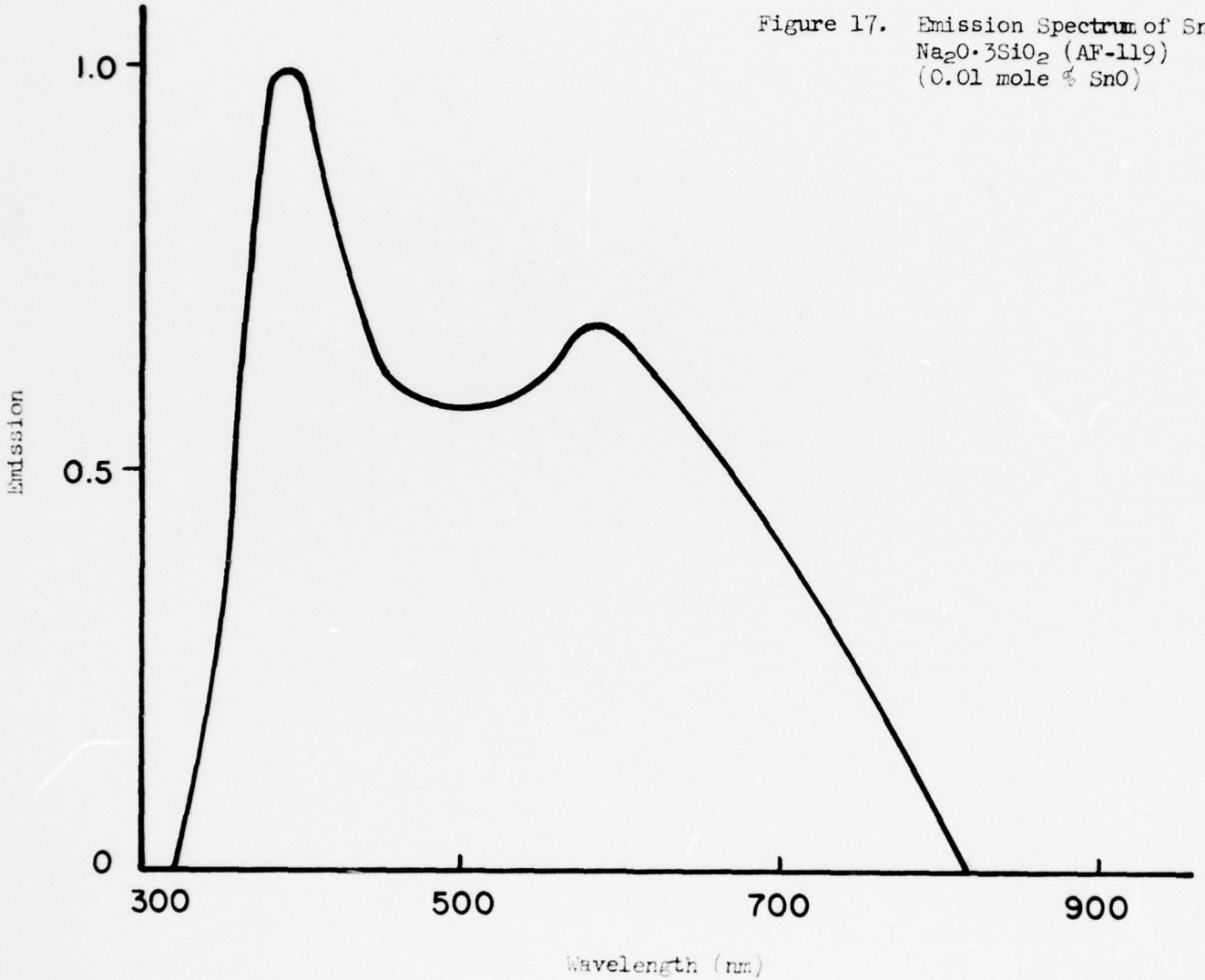

Figure 17. Emission Spectrum of Sn^{2+} in $Na_2O \cdot 3SiO_2$ (AF-119) (0.01 mole % SnO)

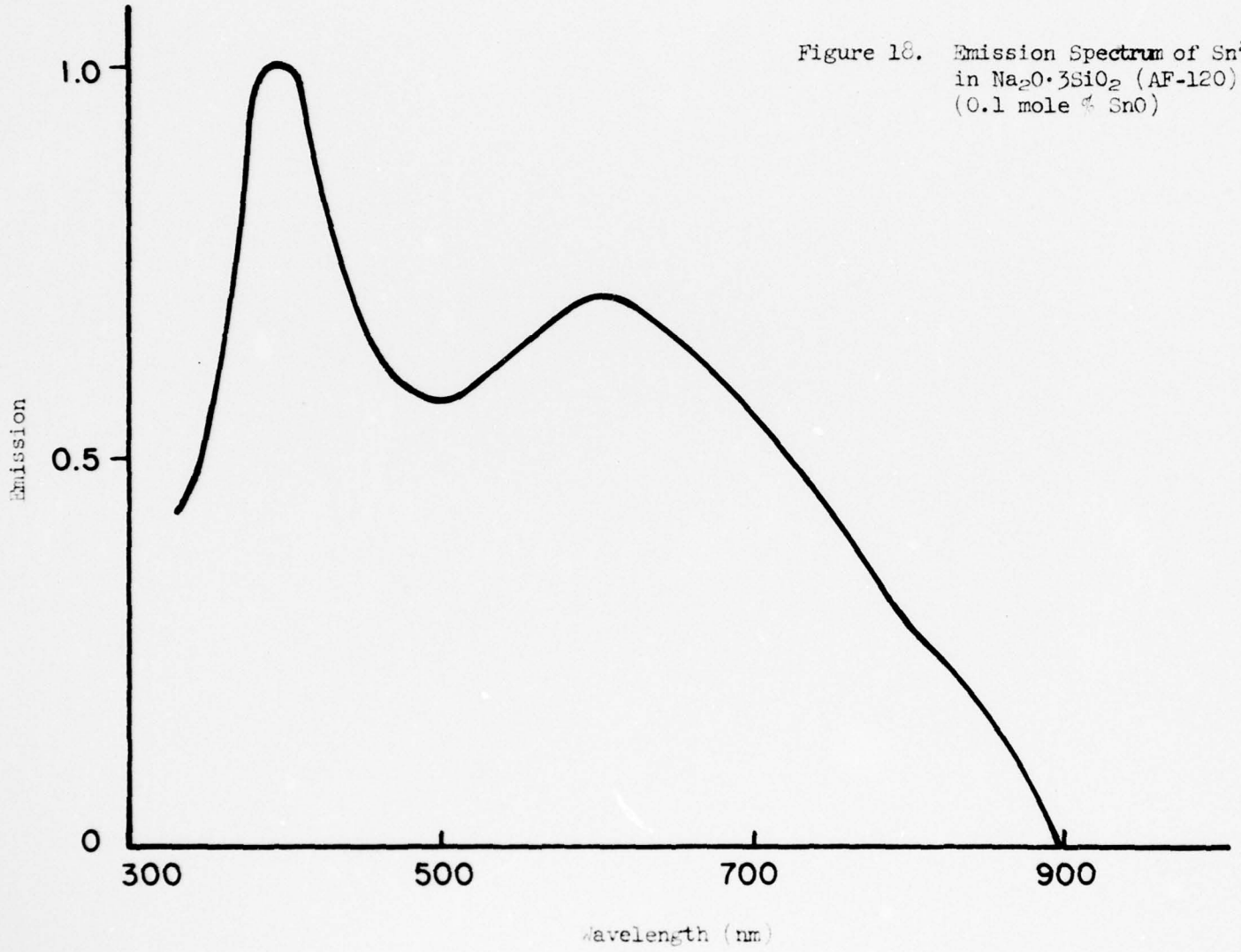

Figure 18. Emission Spectrum of Sn^{2+} in $Na_2O \cdot 3SiO_2$ (AF-120) (0.1 mole % SnO)

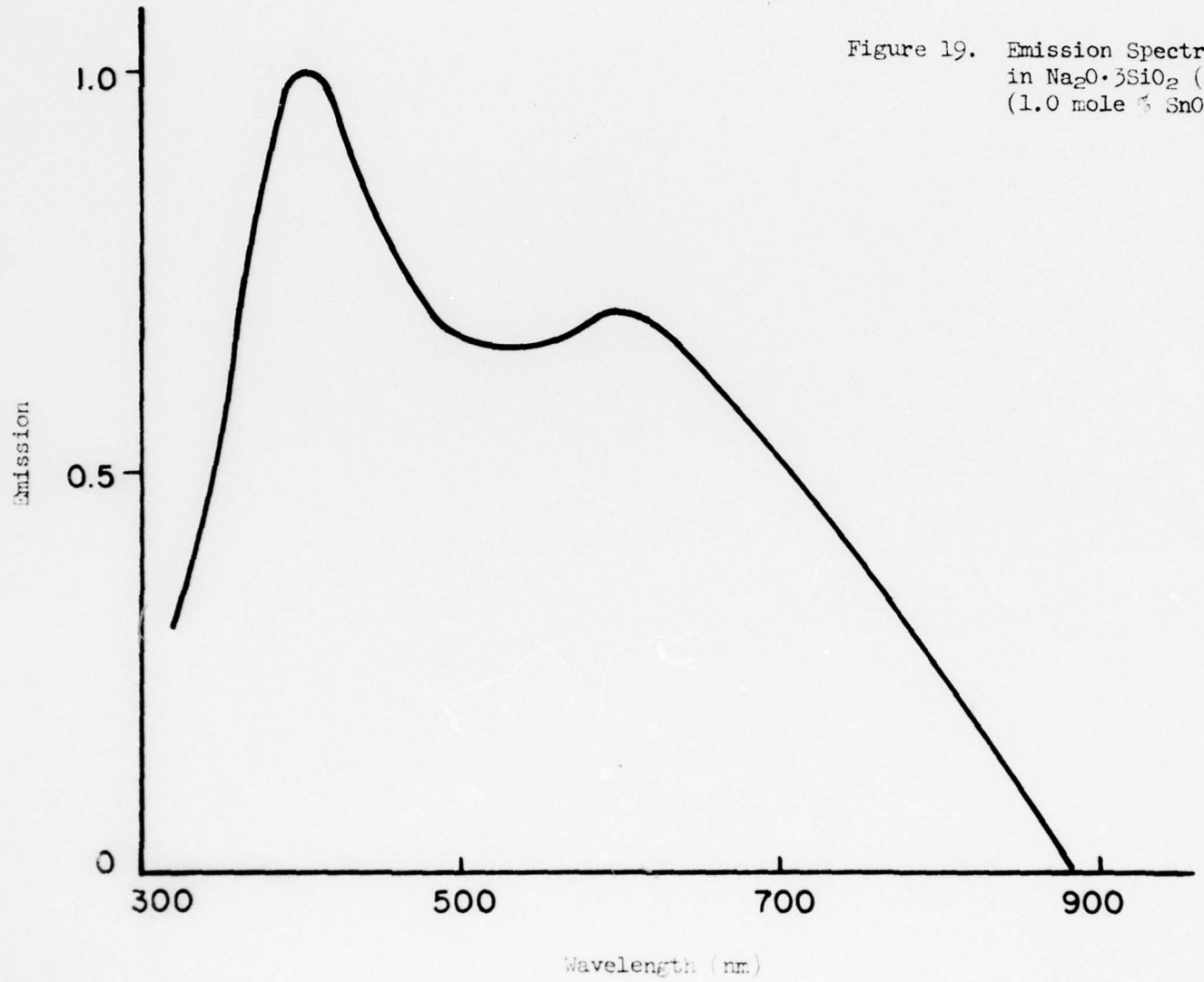

Figure 19. Emission Spectrum of Sn^{2+} in $Na_2O \cdot 3SiO_2$ (AF-121) (1.0 mole % SnO)

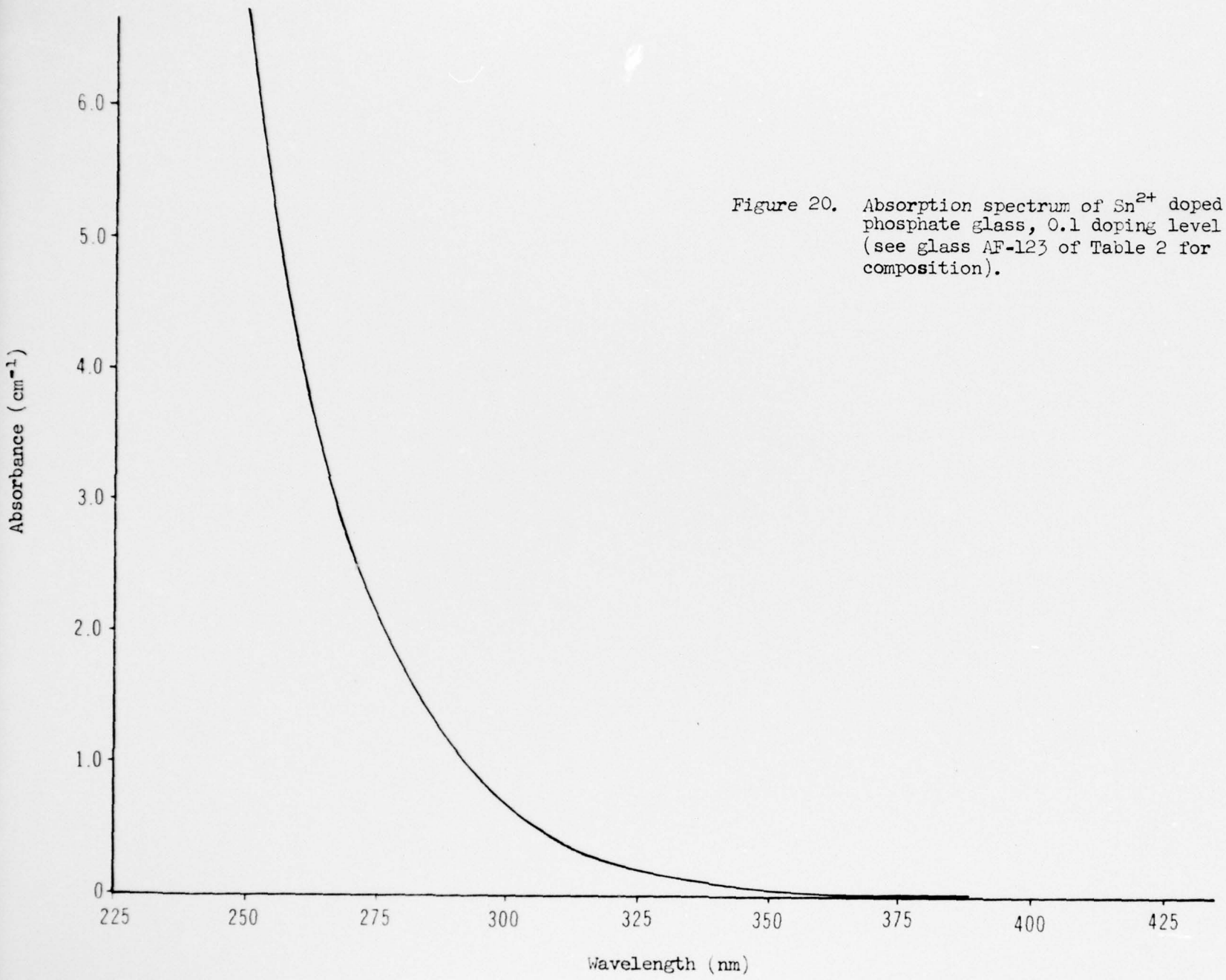

Figure 20. Absorption spectrum of Sn^{2+} doped phosphate glass, 0.1 doping level (see glass AF-123 of Table 2 for composition).

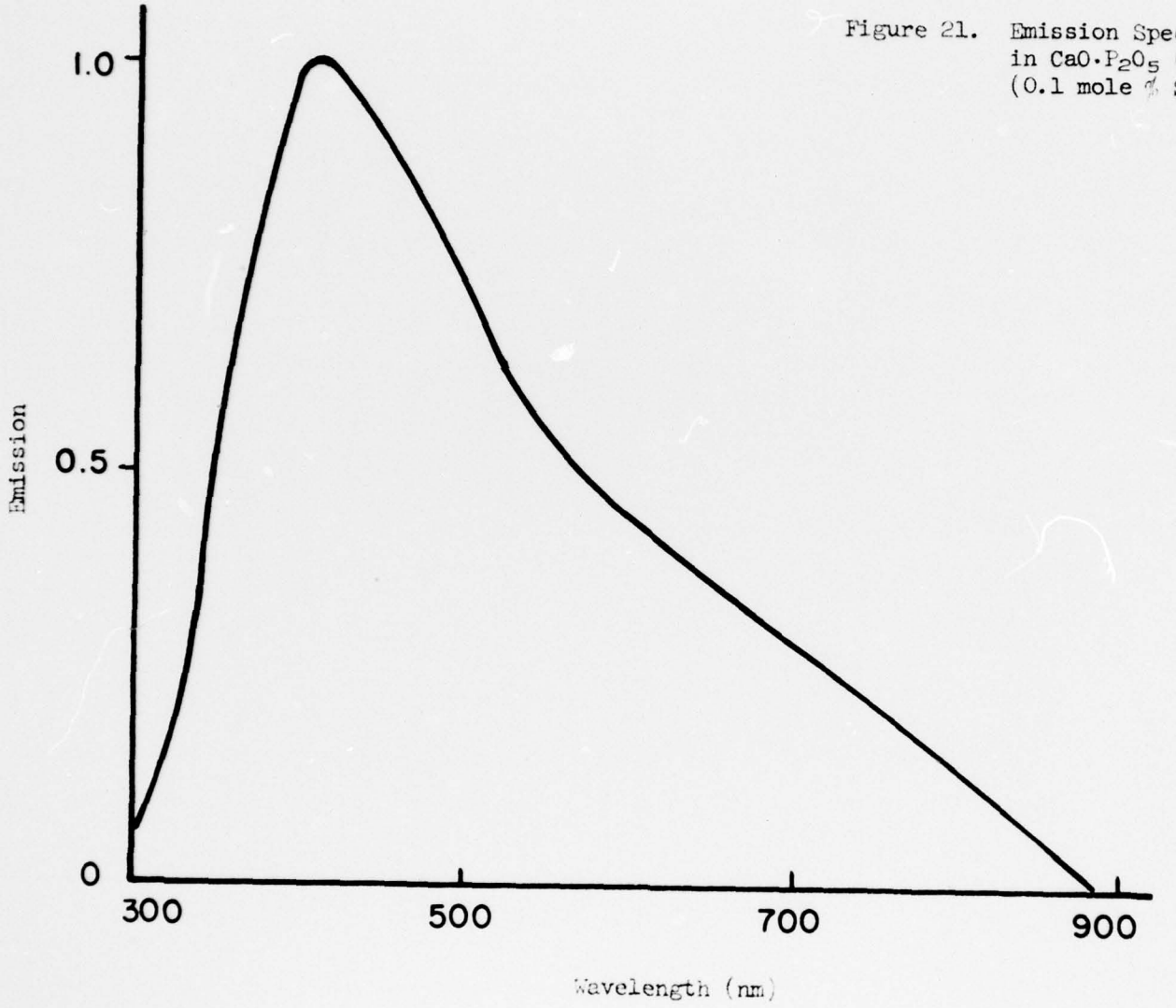

Figure 21. Emission Spectrum of Sn^{2+} in $CaO \cdot P_2O_5$ (AF-123) (0.1 mole % SnO)

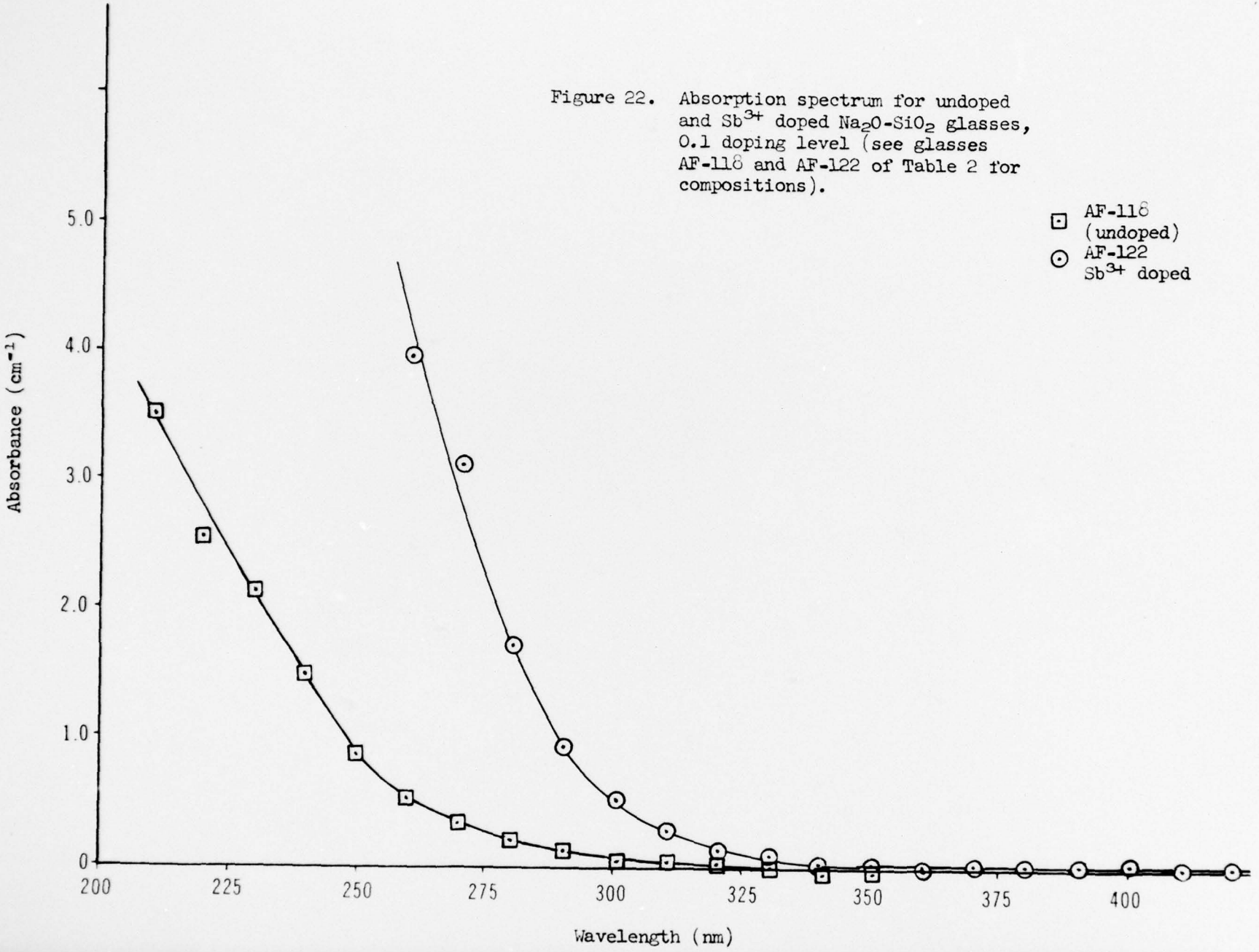

Figure 22. Absorption spectrum for undoped and Sb^{3+} doped Na_2O-SiO_2 glasses, 0.1 doping level (see glasses AF-118 and AF-122 of Table 2 for compositions).